

Synthesis of mesoporous iridium nanosponge: A highly active, thermally stable and efficient olefin hydrogenation catalyst

Sourav Ghosh, Balaji R. Jagirdar*

Department of Inorganic and Physical Chemistry, Indian Institute of Science, Bangalore, Karnataka-560012, India

Email address: jagirdar@ipc.iisc.ernet.in

Table of contents

Figure S1. Experimental Section: Turn over frequency calculation and H ₂ -TPD experimental details including H ₂ -TPD profile of iridium nanosponge, determination of surface exposed iridium metal.....	S2-S4
Table S1. Hydrogenation of alkenes at different temperatures	S5
Table S2. Hydrogenation of 4-vinylcyclohexene by iridium nanosponge	S5
Figure S2. BF TEM images of iridium nanosponge annealed at a) 150 °C for 3 h and b) 300 °C for 3 h, c) powder XRD stack plot of annealed sample with as prepared sample	S6
Table S3. Hydrogenation of styrene using iridium nanosponge annealed at different temperatures	S6
Figure S3. a) BF-TEM image, b) HRTEM image, c) powder XRD stack plot of Ir@BNH _x polymer and iridium nanosponge, and d) FTIR spectra of iridium nanoparticle stabilized by BNH _x polymer (Ir@BNH _x) synthesized from [Ir(COD)Cl] ₂	S7
Figure S4. a) SEM image, b) BF TEM image, c) HRTEM image, d) PXRD pattern, e) FT-IR spectral comparison plot, f) STEM HAADF image (scale bar 1 micron) and g) STEM EDS elemental mapping (scale bar 1 micron) of iridium nanosponge synthesized from IrCl ₃	S7
Figure S5. a) SEM image, b) BF TEM image, c) HRTEM image, d) PXRD pattern, e) FT-IR spectral comparison plot, f) STEM BF image (scale bar 600 nm) and g) STEM EDS	

elemental mapping (scale bar 600 nm) of iridium nanosponge synthesized from [Ir(COD)Cl] ₂	S8
Figure S6. BET isotherms of iridium nanosponge synthesized from a) IrCl ₃ and b) [Ir(COD)Cl] ₂	S8
Table S4. Hydrogenation of styrene using iridium nanosponge prepared from different iridium precursors	S9
Table S5. Surface area, pore size, and pore volume of iridium nanosponges synthesized from different iridium precursors	S9
Figure S7. PXRD stack plot of dried filtrates obtained after the hydrolysis reaction of three different Ir@BNH _x nanocomposites	S10
Figure S8. FT-IR spectral stack plot of dried filtrates obtained after the hydrolysis reaction of three different Ir@BNH _x nanocomposites	S10
Figure S9. ¹¹ B NMR spectral stack plot of dried filtrates obtained after the hydrolysis reaction of three different Ir@BNH _x nanocomposites	S11
Figure S10. FT-IR spectrum of iridium nanosponge treated with CO	S11
GC-MS and ¹H NMR spectral plots	S12-S52

EXPERIMENTAL SECTION

Turnover frequency calculation and H₂-TPD experiment

Temperature programmed desorption (H₂-TPD) experiment was performed with a multipurpose unit coupled to a quadrupole mass spectrometer (BELCAT II catalyst analyser, Japan). The H₂-TPD profile was given below (Fig. S1). It contains two peaks, one at 170 °C and other one appears at 395 °C. The first peak at 170 °C could be ascribed to desorption of weakly bound hydrogen from the metal surface whereas, broad peak at 395 °C refers to the strongly bound hydrogen on metallic iridium.

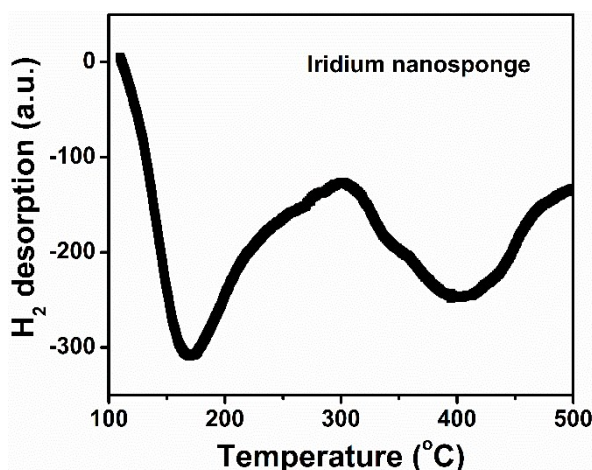


Figure S1. H₂-TPD profile of iridium nanosponge.

Based on the BET surface area data and H₂-TPD profile, we have calculated the fraction of iridium site is exposed for catalysis. Few assumptions were made for the calculation which are:

1. Since, iridium nanosponge is mesoporous in nature, then all the exposed iridium atoms takes part in the catalysis step. There is no hindered diffusion as the pore size varies between 5-100 nm with a peak centered at 27.7 nm (Fig. 1g; main manuscript).
2. The iridium lattice possess FCC (face-centred cubic) crystal structure. According to the surface energy value, the most atomically dense lattice plane (111) is having lowest surface energy among the other lattice planes ((110) and (100)). We assume that, only (111) lattice plane which is having lowest surface energy is exposed for iridium.

The FCC unit cell edge length for iridium is 3.833 Å.

The area occupied by (111) lattice plane of a FCC lattice is = $\frac{a^2 \times \sqrt{3}}{2}$, where a is the unit cell edge length (3.833 Å). The area was calculated to be $1.2724 \times 10^{-19} \text{ m}^2$. The total occupancy for (111) lattice plane for a FCC system is 2 atom.

Therefore, $1.2724 \times 10^{-19} \text{ m}^2$ of surface area contains 2 atoms;

33.5 m²/g (BET surface area) contains 3.8668×10^{20} atoms.

1 gm of iridium, with a surface area of 33.5 m²/g have 3.86668×10^{20} atoms exposed. Upon dividing with Avogadro's number ($N_A = 6.022 \times 10^{23} \text{ mol}^{-1}$), 1 gm of iridium nanosponge was found to have 0.8734 mmol of iridium exposed.

Deconvolution of H₂-TPD profile shows that, 0.337 mmol/g of hydrogen (which is strongly bound to the iridium surface) was desorbed from the iridium nanosponge. Since, each iridium atom can bind with single hydrogen atom [$\text{Ir (s)} + \frac{1}{2} \text{H}_2 \text{ (g)} = \text{IrH (s)}$], then 0.674 mmol ($2 \times 0.337 \text{ mmol}$) of hydrogen atom was actually bound with the iridium metal. Now, assuming 1:1 stoichiometric binding of iridium and hydrogen, the exposed iridium atom concentration was calculated to be 0.674 mmol for 1 gm of iridium. But, from BET surface area measurement, the exposed iridium concentration was measured to be 0.8734 mmol for 1 gm of iridium. The lower value obtained from H₂-TPD experiment could be attributed to the fact that, all the iridium surface was not covered by (111) lattice plane. There are low density planes such as (110) and (100) present at the surfaces which causes decrement in the amount of hydrogen adsorption.

Turnover frequency was calculated on the basis of total iridium atom exposed (obtained from H₂-TPD experiment).

Turnover frequency (TOF) = moles of substrate transformed per mole of iridium per hour (for total metal)

Determination of concentration of surface exposed iridium metal

H₂-TPD study reveals that, 0.674 mmol of iridium is exposed at the surface per gram of iridium. Since, 0.05 mol% (0.01 mmol) iridium catalyst is the optimized catalyst concentration used for most of the hydrogenation reactions, the concentration of the surface exposed iridium was calculated for this particular concentration.

5.2 mmol (1 gm) of iridium has 0.674 mmol of surface exposed iridium atoms.

Then, 0.01 mmol of iridium has $\frac{0.674 \times 0.01}{5.2} = 0.0013$ mmol of surface exposed iridium atoms.

Therefore, the surface atoms exposed for 0.01 mmol of iridium is $(0.0013/0.01) = 13 \%$.

In parenthesis; Turnover frequency (TOF) = moles of substrate transformed per mole of exposed iridium per hour (for exposed metal)

Table S1. Hydrogenation of alkenes at different temperatures

Entry	Substrate	Solvent	T (°C)	Time (h)	Conv. (%) ^a	TOF (h ⁻¹) ^b
1	Styrene	CH ₂ Cl ₂	30	4	>99	500 (3846)
2	Styrene	n-heptane	30	1.75	>99	1143 (8791)
3	Styrene	n-heptane	50	0.75	>99	2667 (20512)
4	Styrene	n-heptane	75	0.42	>99	4762 (36630)
5	Cyclohexene	CH ₂ Cl ₂	30	4	>99	500 (3846)
6	Cyclohexene	n-heptane	75	0.4	>99	5000 (38461)
7	1-Hexadecene	CH ₂ Cl ₂	30	6	>99	333 (2564)
8	1-Hexadecene	n-heptane	75	0.3	>99	6667 (51282)

Substrate/iridium catalyst ratio was 2000 and 4 bar hydrogen gas pressure was maintained for all the reactions; ^aconversion determined by GC/MS analysis; ^bturnover frequency = mol (alkene)/mol (Ir nanosponge)·h based on total metal, in parenthesis based on available surface atoms of catalyst.

Table S2. Hydrogenation of 4-vinylcyclohexene by iridium nanosponge

Entry	Substrate	Time (h)	Conv. (%) ^a	TOF (h ⁻¹) ^b	Product
1	4-Vinylcyclohexene	3	26.5 ^c	177 (1359)	Ethyl cyclohexane
2	4-Vinylcyclohexene	6	58.3 ^c	194 (1495)	Ethyl cyclohexane

All reactions were carried out at a constant temperature of 30 °C and constant hydrogen gas pressure of 4 bar in CH₂Cl₂; ^aconversion determined by GC/MS analysis, ^bturnover frequency = mol (ethyl cyclohexane)/mol (Ir nanosponge) h, in parenthesis based on available surface atoms of catalyst; ^cconversion of 4-vinylcyclohexene to ethylcyclohexane.

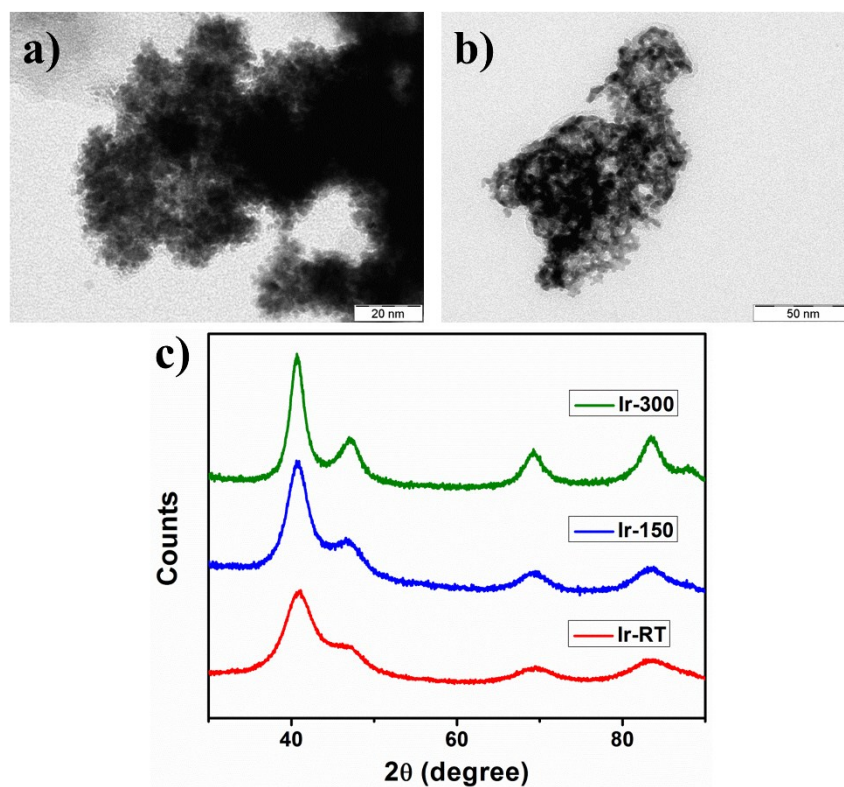


Figure S2. BF TEM images of iridium nanosponge annealed at a) 150 °C for 3 h and b) 300 °C for 3 h, c) powder XRD stack plot of annealed sample with as prepared sample.

Table S3. Hydrogenation of styrene using iridium nanosponge annealed at different temperatures

Entry	Catalyst	Time (h)	Conversion (%) ^a	TOF (h ⁻¹) ^b
1	Ir-RT ^c	4	>99	500
2	Ir-150	4	>99	500

All reactions were carried out at fixed styrene/iridium catalyst ratio of 2000 (20 mmol of styrene and 0.01 mmol of iridium nanosponge), 4 bar of hydrogen gas pressure, and at 30 °C in CH₂Cl₂; ^aconversion determined by GC/MS analysis; ^bturnover frequency = mol (product)/mol (Ir nanosponge)-h; ^cIridium nanosponge as prepared sample (without any heat treatment).

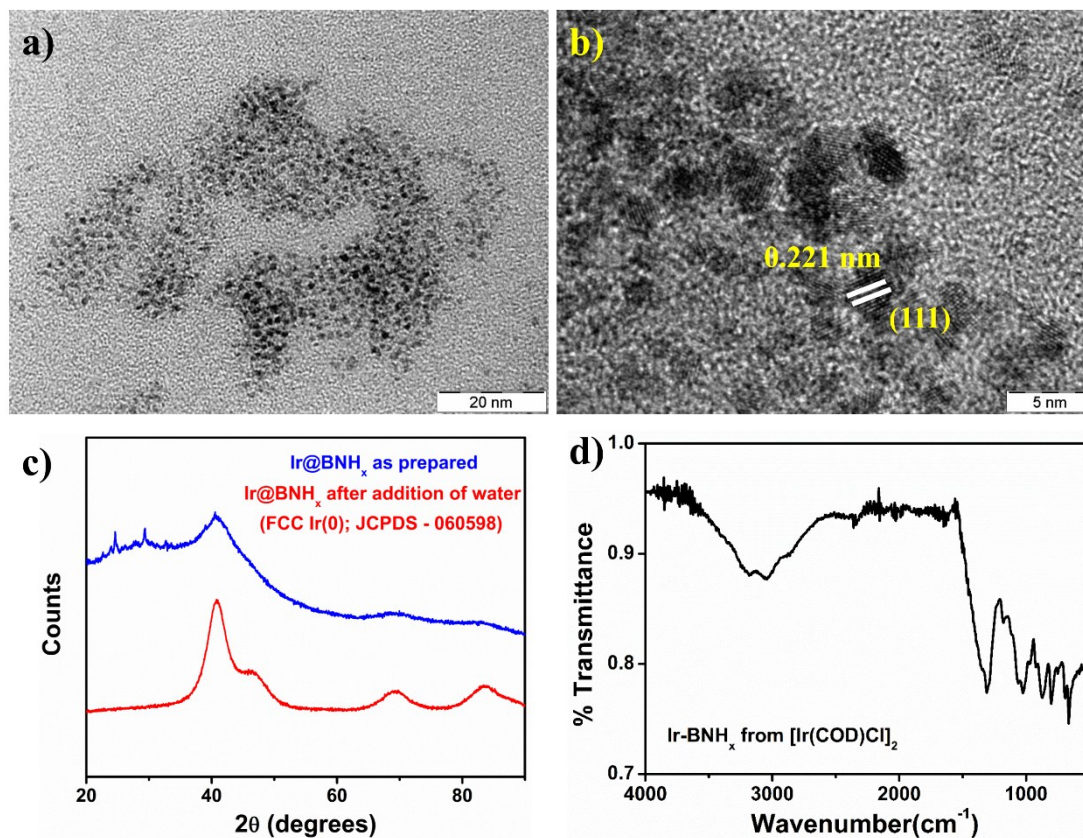


Figure S3. a) BF-TEM image, b) HRTEM image, c) powder XRD stack plot of Ir@BNH_x polymer and iridium nanosponge, and d) FTIR spectra of iridium nanoparticle stabilized by BNH_x polymer (Ir@BNH_x) synthesized from [Ir(COD)Cl]₂.

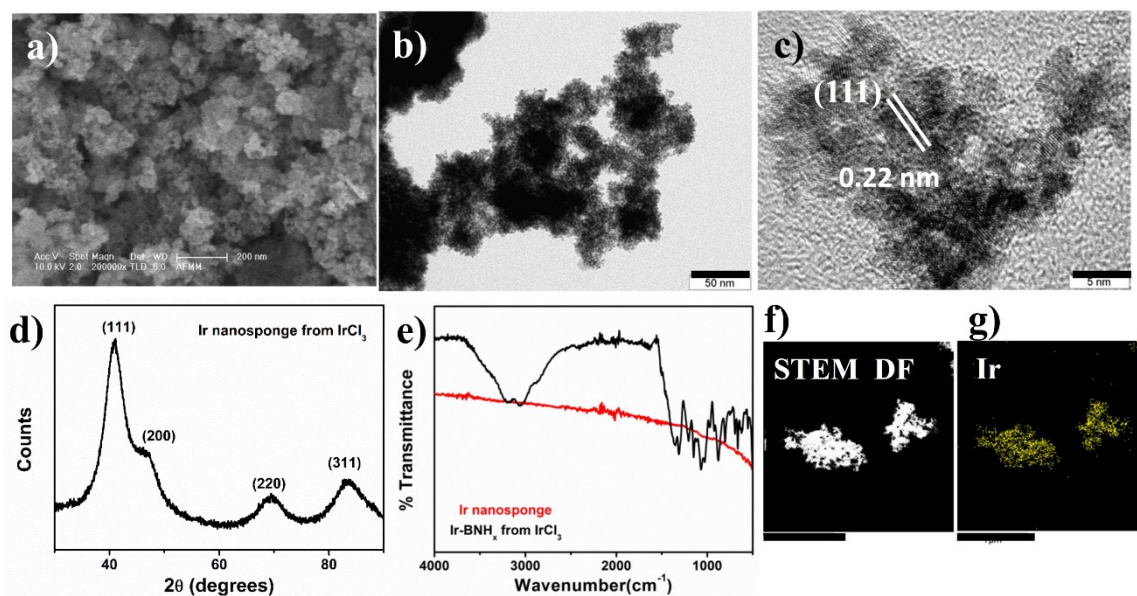


Figure S4. a) SEM image, b) BF TEM image, c) HRTEM image, d) PXRD pattern, e) FT-IR spectral comparison plot, f) STEM HAADF image (scale bar 1 micron) and g) STEM EDS elemental mapping (scale bar 1 micron) of iridium nanosponge synthesized from IrCl_3 .

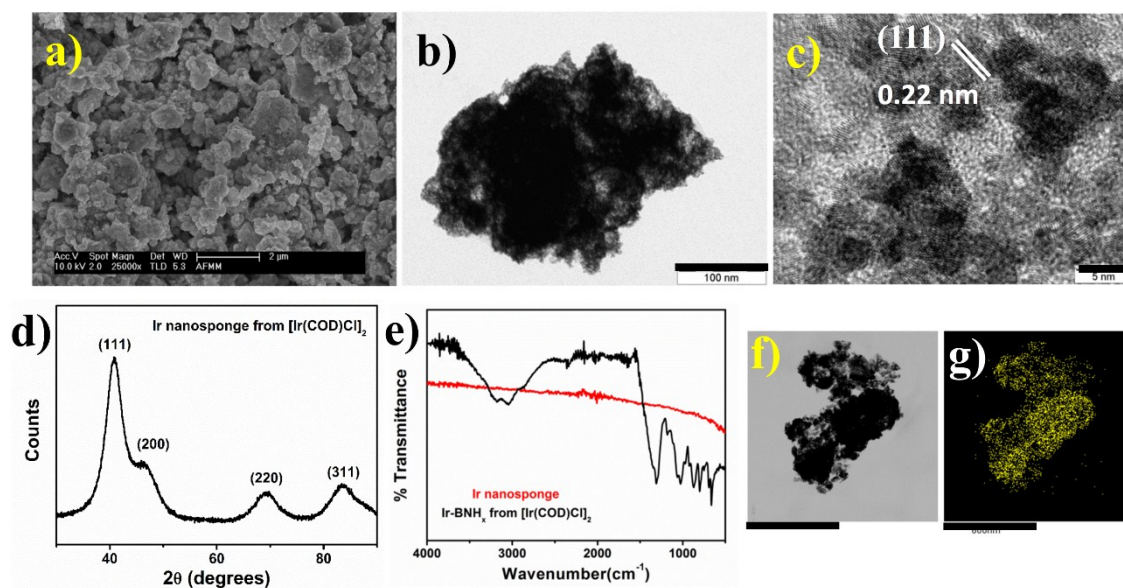


Figure S5. a) SEM image, b) BF TEM image, c) HRTEM image, d) PXRD pattern, e) FT-IR spectral comparison plot, f) STEM BF image (scale bar 600 nm) and g) STEM EDS elemental mapping (scale bar 600 nm) of iridium nanosponge synthesized from $[\text{Ir}(\text{COD})\text{Cl}]_2$.

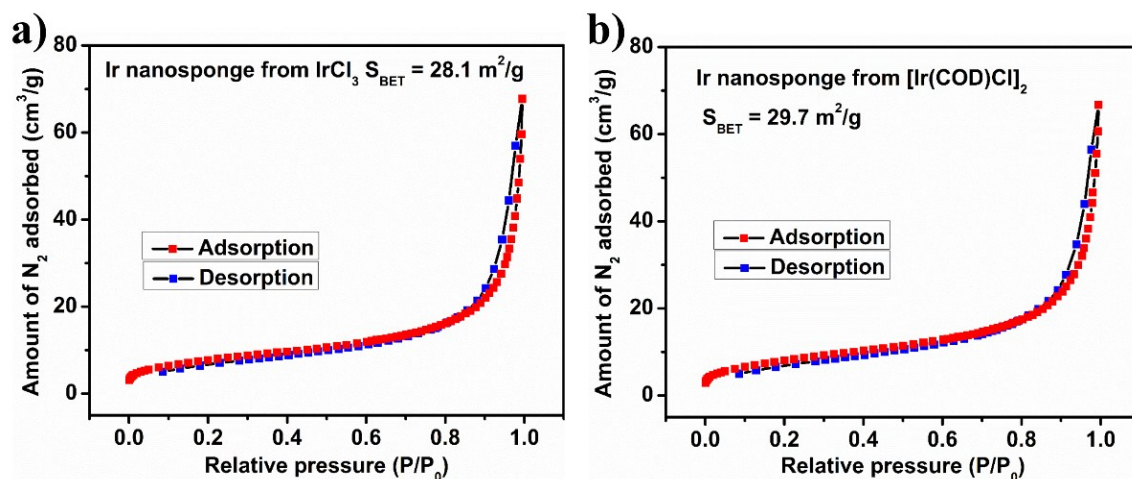


Figure S6. BET isotherms of iridium nanosponge synthesized from a) IrCl_3 and b) $[\text{Ir}(\text{COD})\text{Cl}]_2$.

Table S4. Hydrogenation of styrene using iridium nanosponge prepared from different iridium precursors

Entry	Styrene/catalyst	Catalyst	Time (h)	Conversion (%) ^a	TOF (h^{-1}) ^b
1	2000	Ir-1 ^c	1 ^f	53.6 ^f	1072
2	2000	Ir-1 ^c	4	>99	500
3	2000	Ir-2 ^d	1 ^f	53.9 ^f	1078
4	2000	Ir-2 ^d	4	>99	500
5	2000	Ir-3 ^e	1 ^f	53.4 ^f	1068
6	2000	Ir-3 ^e	4	>99	500

All reactions were carried out at 4 bar hydrogen gas pressure and at 30 °C in CH_2Cl_2 ; ^aconversion determined by GC/MS analysis; ^bturnover frequency = mol (styrene)/mol (Ir nanosponge) h; ^ciridium catalyst prepared from H_2IrCl_6 ; ^diridium catalyst prepared from $\text{IrCl}_3 \cdot x\text{H}_2\text{O}$; ^eiridium catalyst prepared from $[\text{Ir}(1,5\text{-COD})\text{Cl}]_2$; ^freaction was stopped after 1 h and aliquot was drawn for $^1\text{H-NMR}$ and GC-MS study, % styrene converted to ethyl benzene.

Table S5. Surface area, pore size, and pore volume of iridium nanosponges synthesized from different iridium precursors

Entry	Materials	S_{BET} (m^2/g)	Pore size (nm)	Pore volume (cm^3/g)
1	Ir from H_2IrCl_6	33.5	27.7	0.245
2	Ir from IrCl_3	28.1	16.7	0.104
3	Ir from $[\text{Ir}(\text{COD})\text{Cl}]_2$	29.7	16.2	0.102

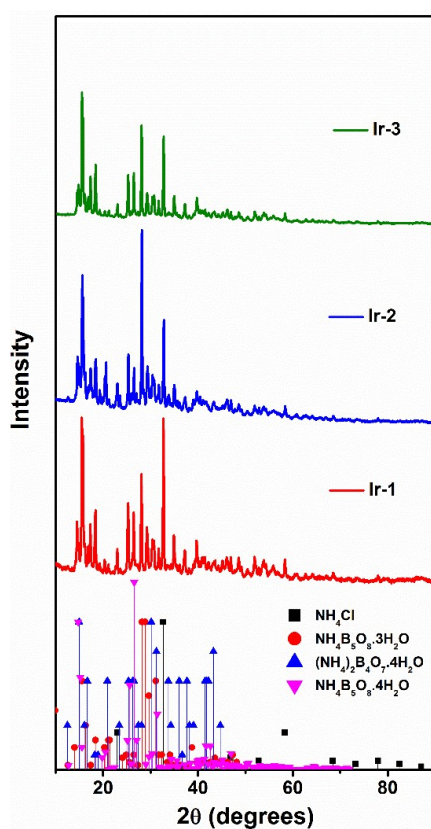


Figure S7. PXR D stack plot of dried filtrates obtained after the hydrolysis reaction of three different $\text{Ir}@\text{BNH}_x$ nanocomposite. The iridium precursors used for synthesis of $\text{Ir}@\text{BNH}_x$ nanocomposite are Ir-1: H_2IrCl_6 , Ir-2: IrCl_3 , and Ir-3: $[\text{Ir}(\text{COD})\text{Cl}]_2$. JCPDS card number:

NH₄Cl: 07-0007; (NH₄)₂B₄O₇·4H₂O: 19-0061; NH₄B₅O₈·4H₂O: 74-1233; NH₄B₅O₈·3H₂O: 12-0637.

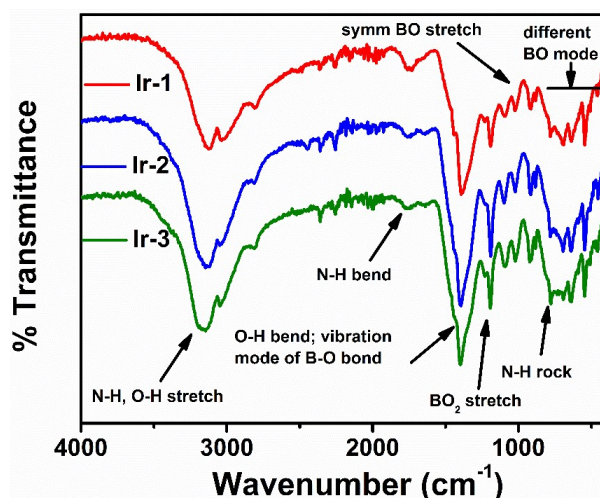


Figure S8. FT-IR spectral stack plot of dried filtrates obtained after the hydrolysis reaction of three different Ir@BNH_x nanocomposite. The iridium precursors used for synthesis of Ir@BNH_x nanocomposite are Ir-1: H₂IrCl₆, Ir-2: IrCl₃, and Ir-3: [Ir(COD)Cl]₂.

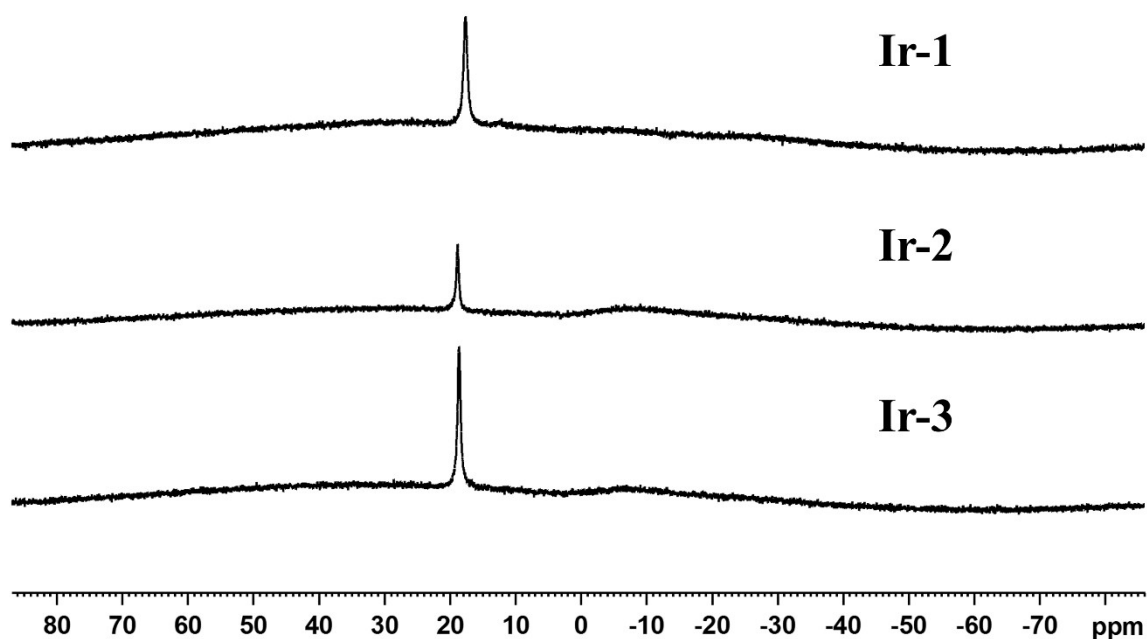


Figure S9. ¹¹B-NMR spectral stack plot of dried filtrates obtained after the hydrolysis reaction of three different Ir@BNH_x nanocomposites. Dried filtrates were dissolved in milli Q water and NMR spectra was recorded. The iridium precursors used for synthesis of Ir@BNH_x nanocomposite are Ir-1: H₂IrCl₆, Ir-2: IrCl₃, and Ir-3: [Ir(COD)Cl]₂.

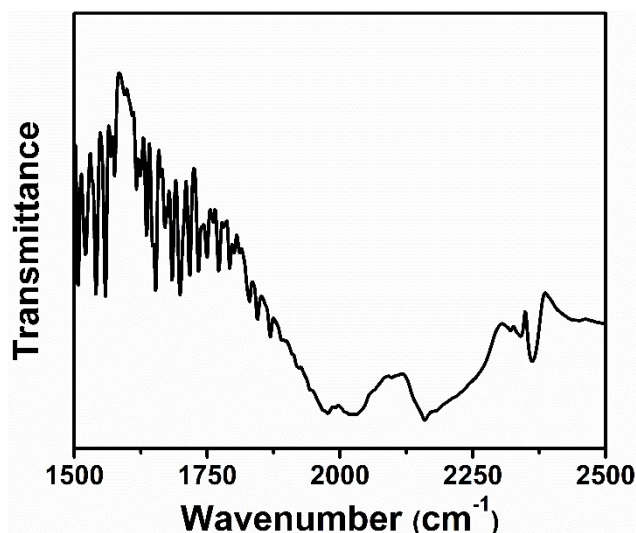
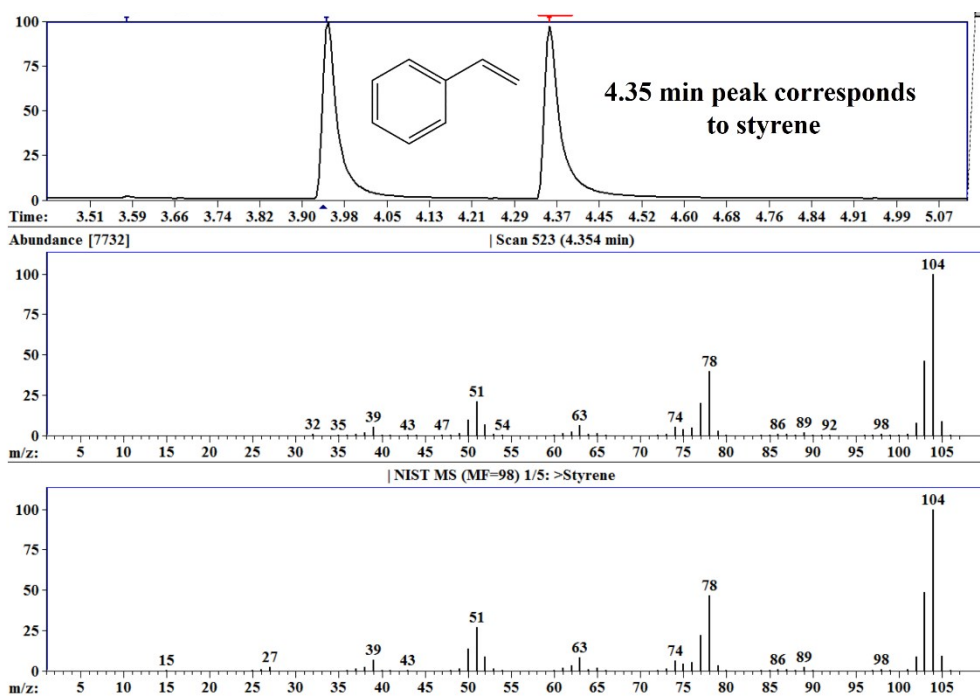


Figure S10. FT-IR spectrum of iridium nanosponge treated with CO.

General information

For optimization study (except table 2, table S1 entry number 6 and 8, and table S2), styrene was used as a model substrate and the product obtained was ethylbenzene. Here, GC-MS characterization of styrene and ethylbenzene were presented first as a model spectra. Afterwards, only gas chromatogram was attached for styrene and ethylbenzene.



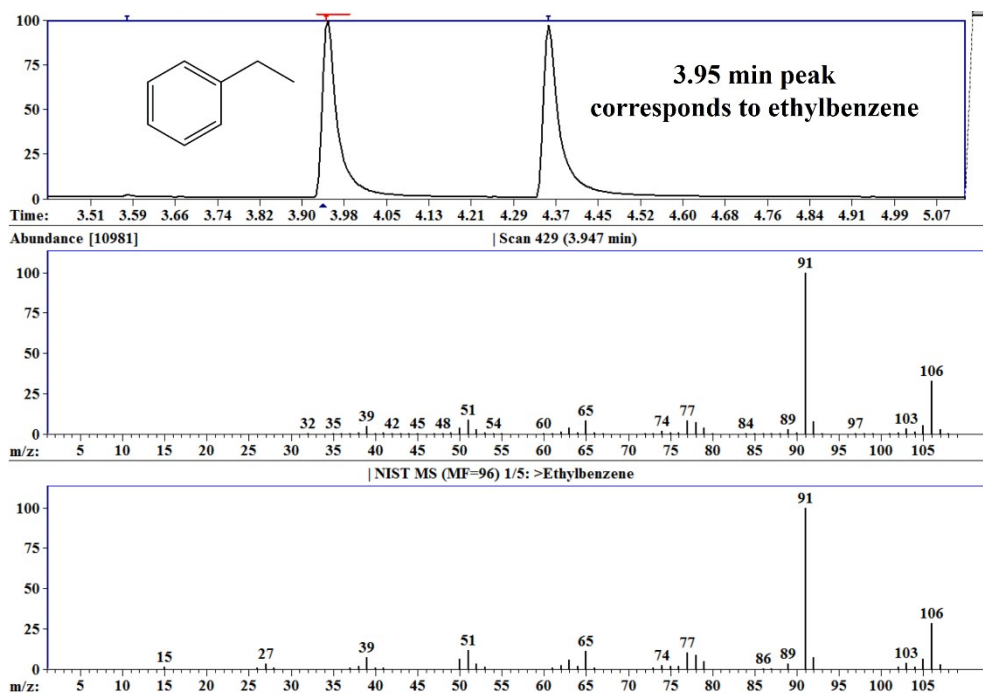
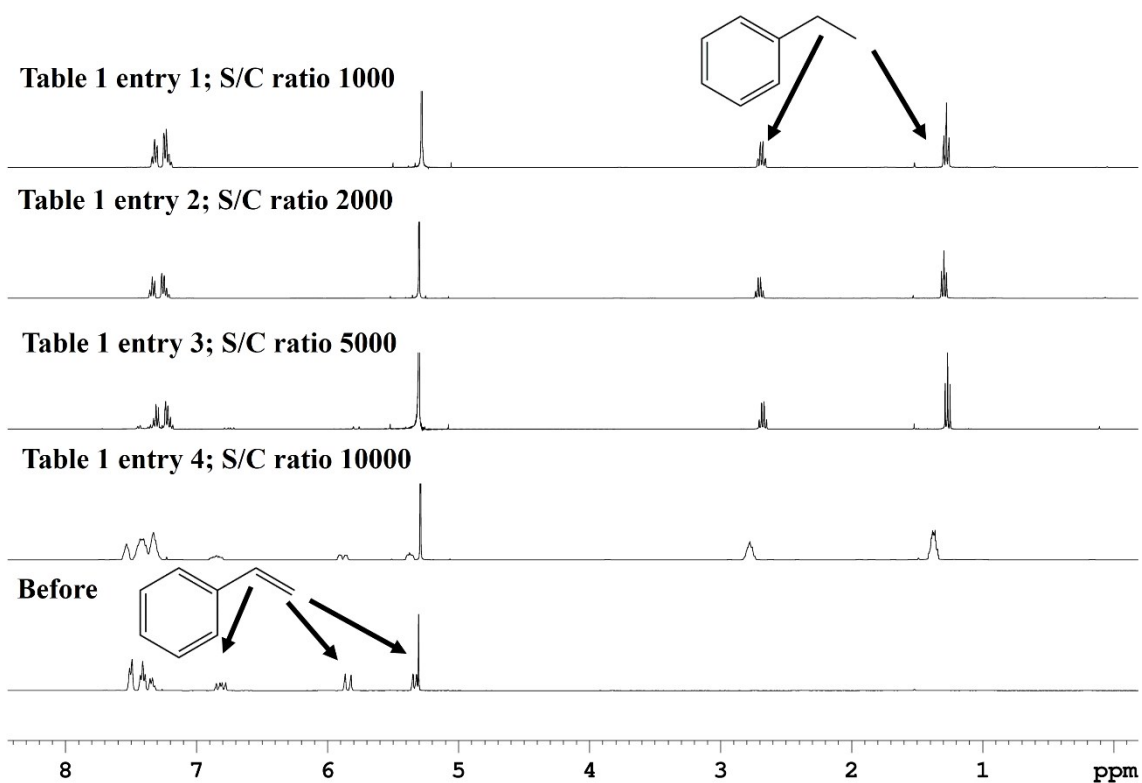


Table 1 (effect of substrate/catalyst ratio) – entry 1-4



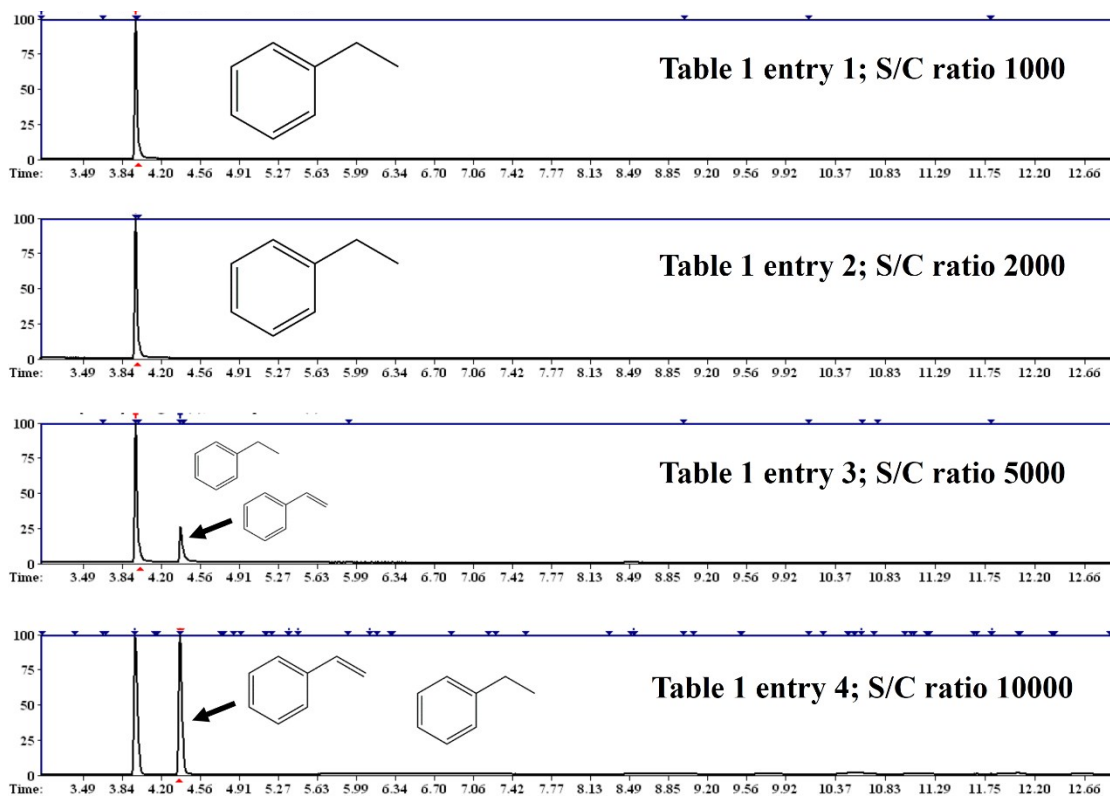
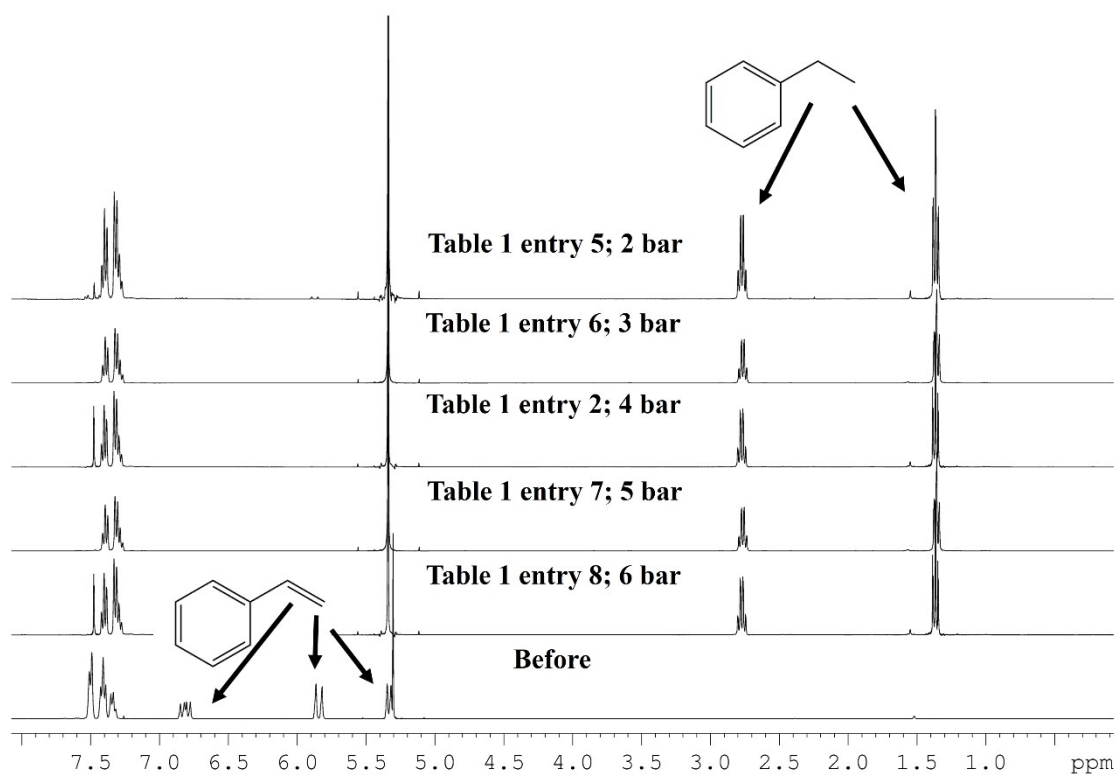
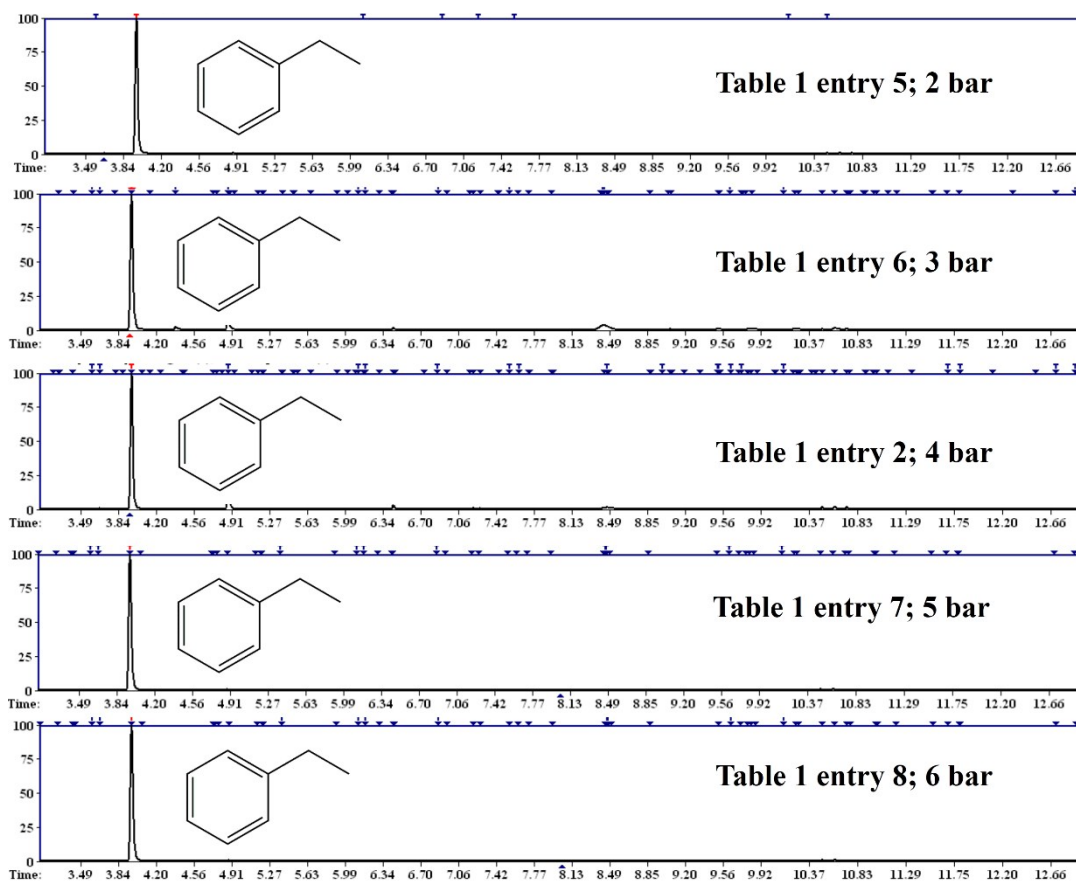


Table 1 (effect of pressure) – entry 5-8





Blank experiment without hydrogen gas:

Gas Chromatogram

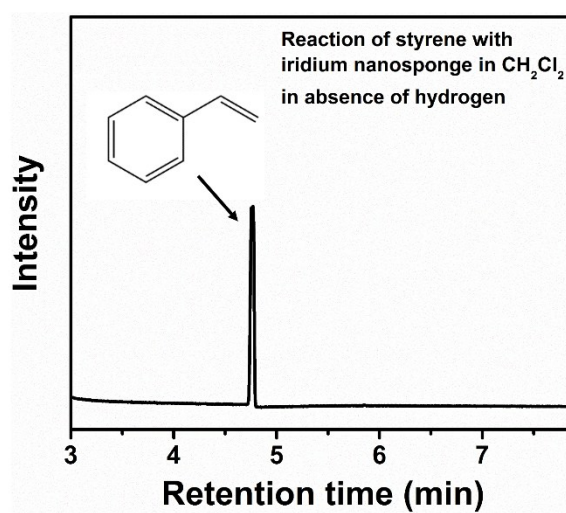
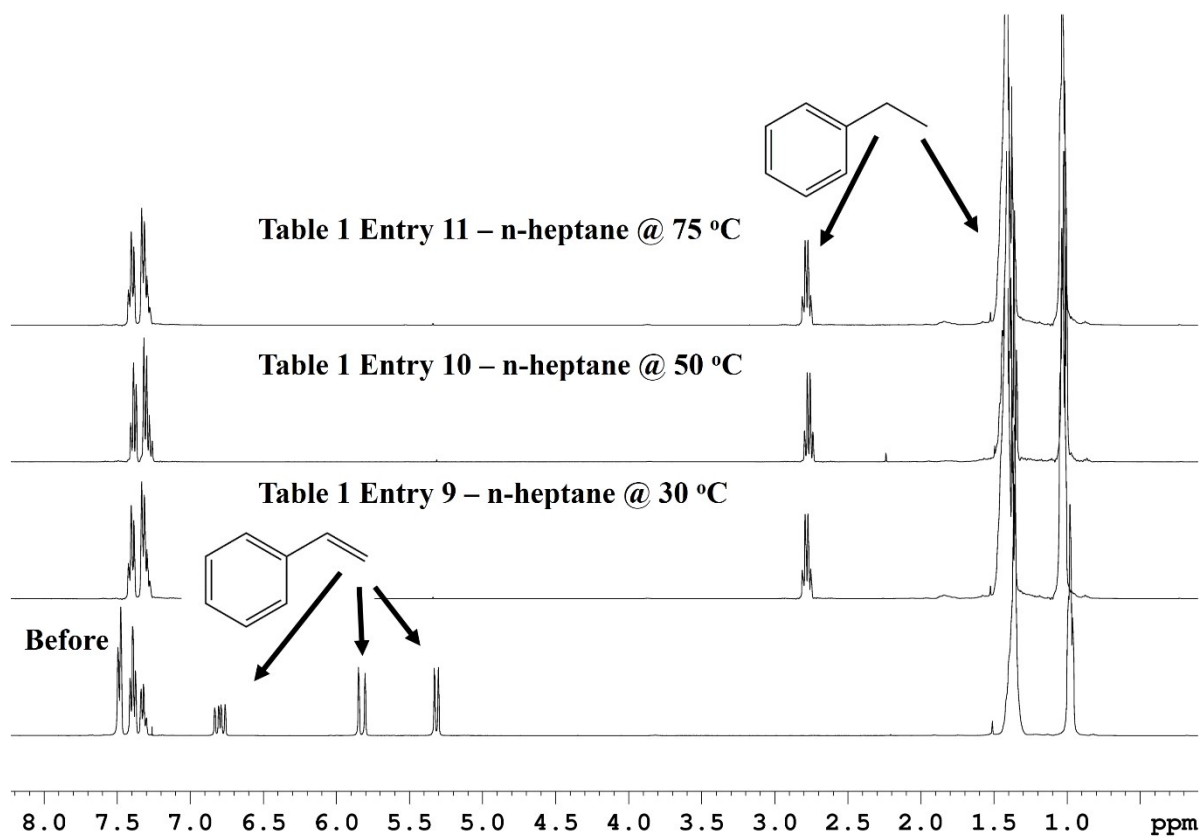


Table 1 (effect of temperature) - entry 9-11



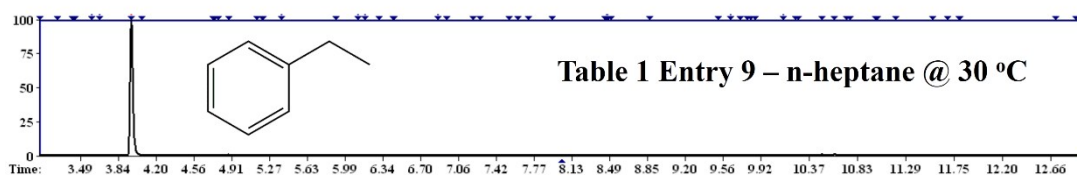
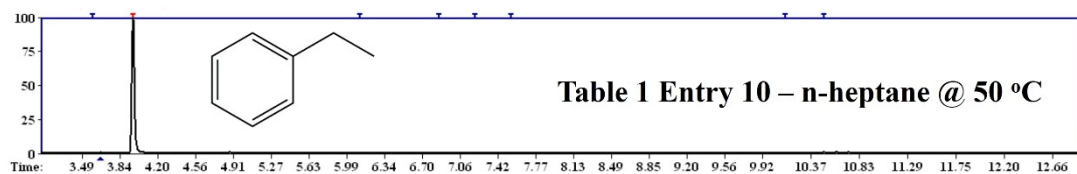
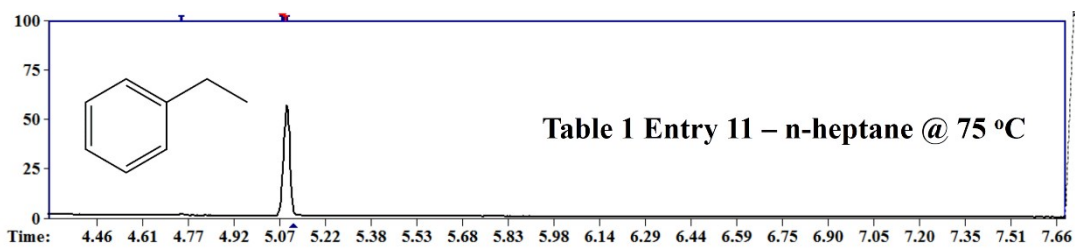
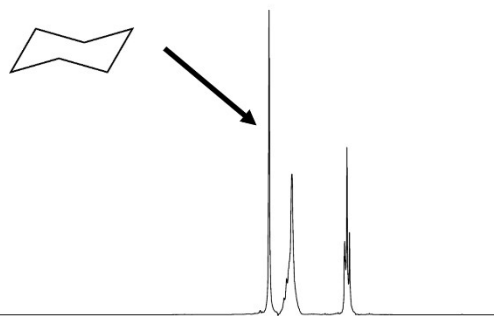


Table S1 (Hydrogenation of alkenes at different temperatures) entry 1-4 is same for the table 1 entry 2, 9-11. Table S1 entry 5 is same for the table 3 entry 9. Similarly, table S1 entry 7 is same for the table 3 entry 7.

Table S1 entry 6 [effect of temperature]

After
Table S1 Entry 6



Before

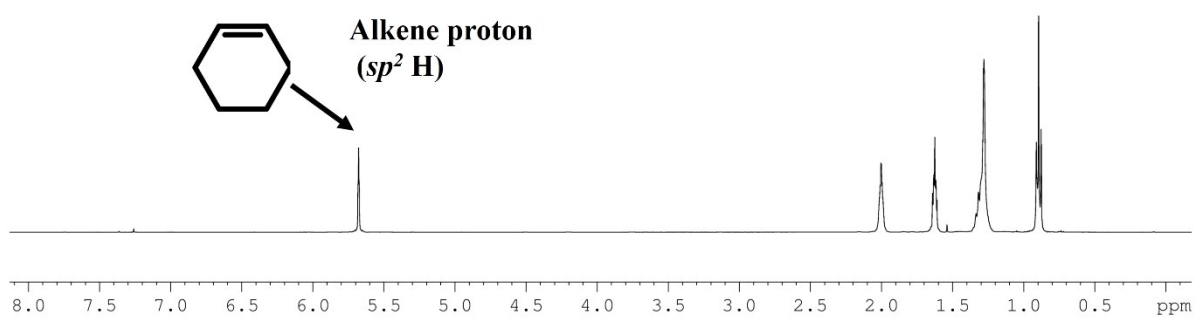
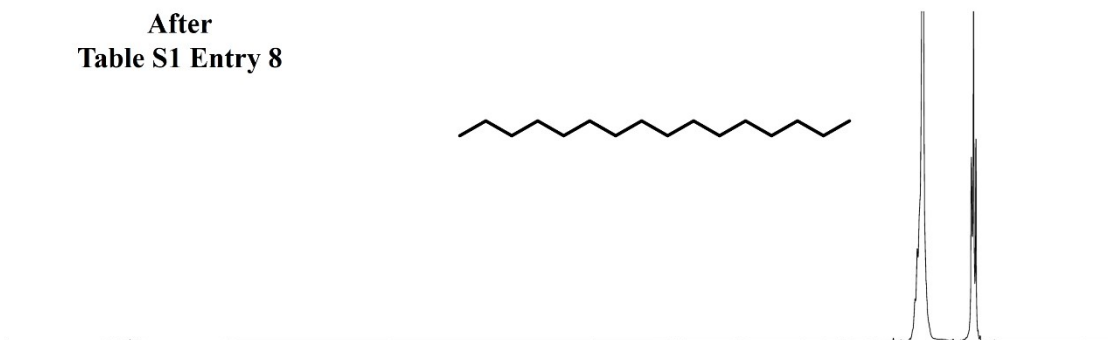
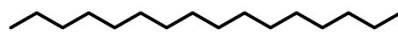
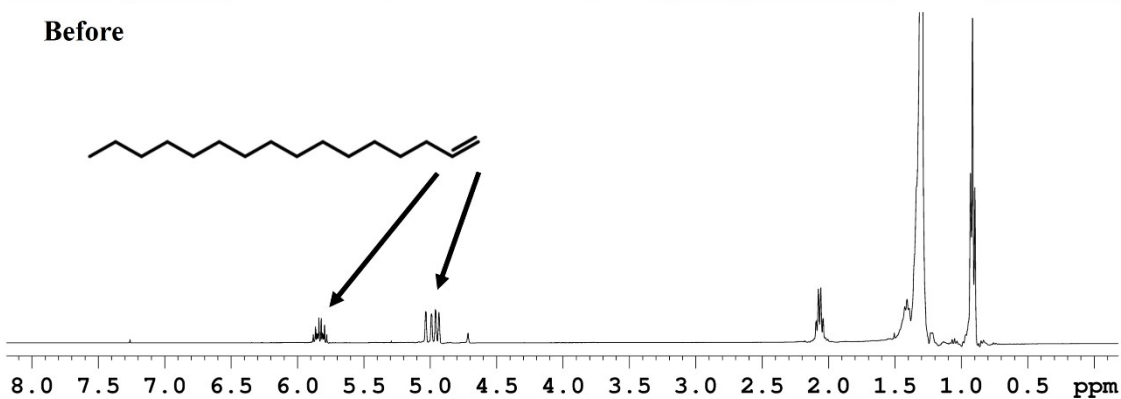
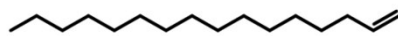


Table S1 entry 8 [effect of temperature]

After
Table S1 Entry 8



Before



After
Table S1 Entry 8

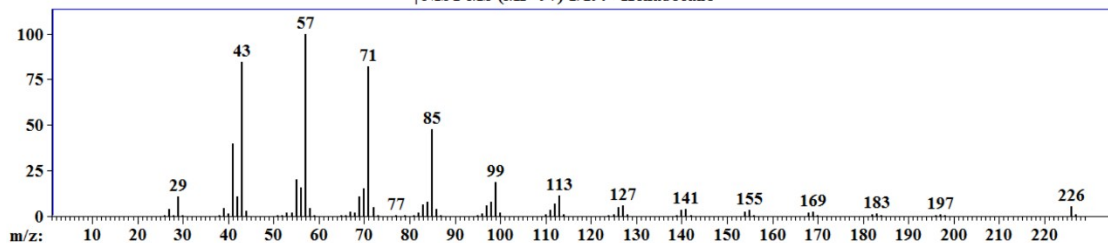
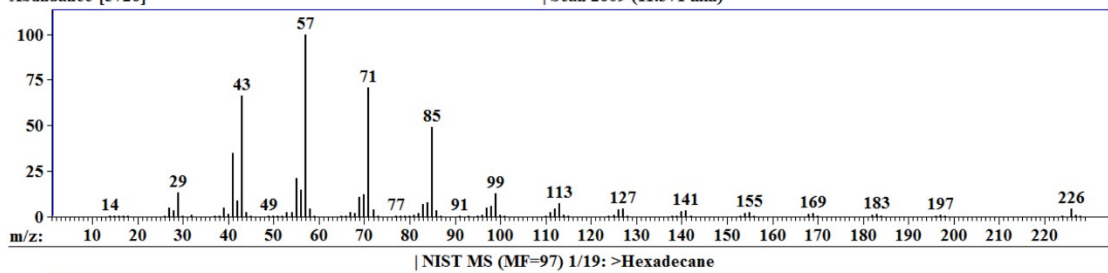
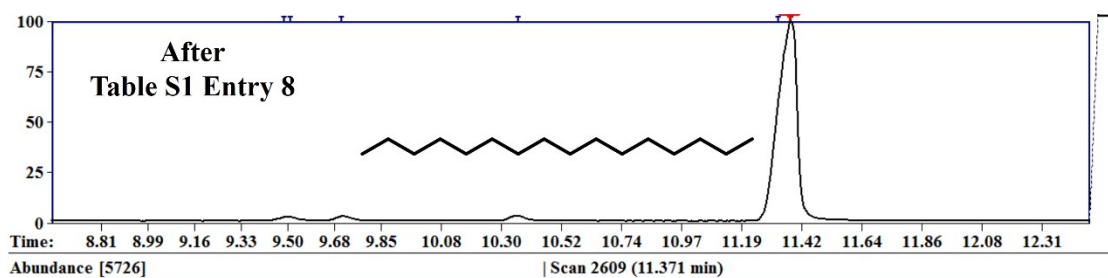
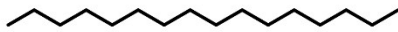


Table 2 entry 1

Table 2 entry 1

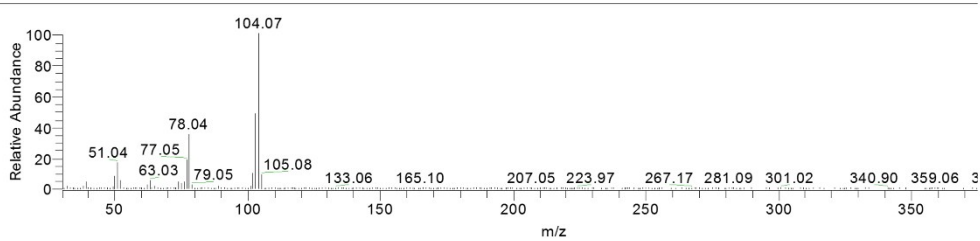
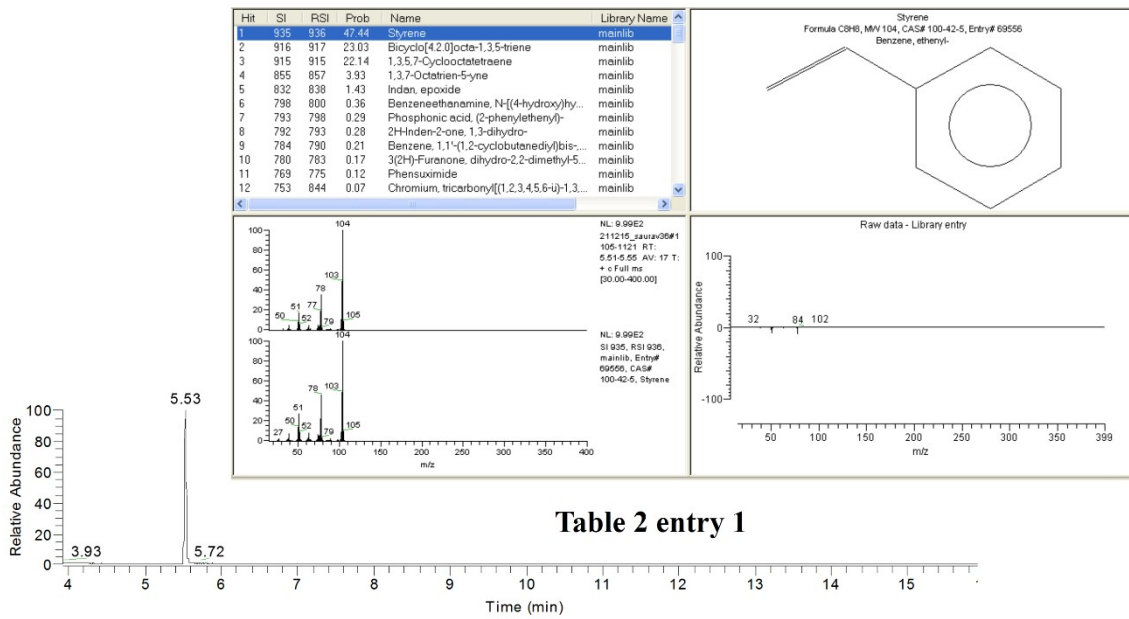
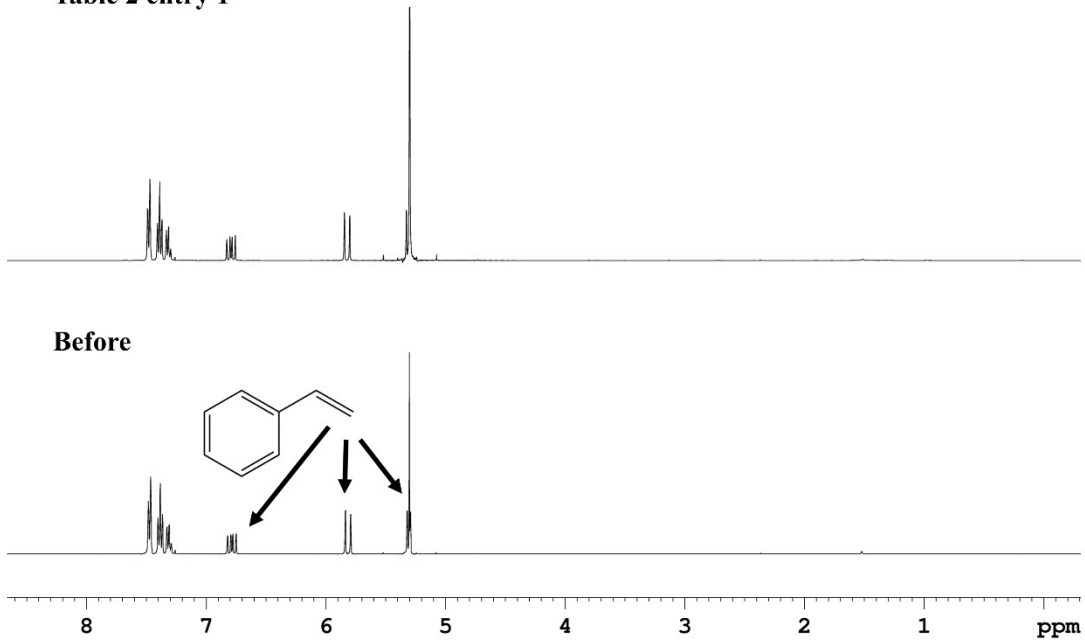
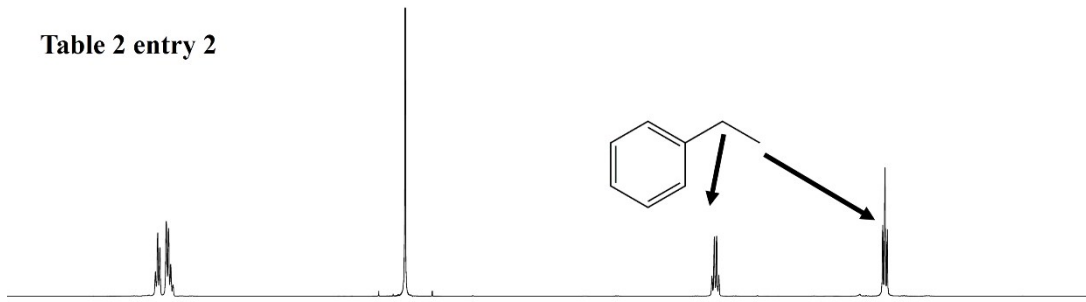
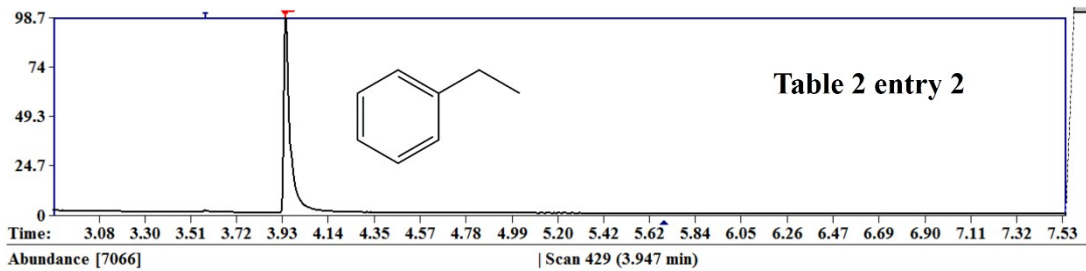
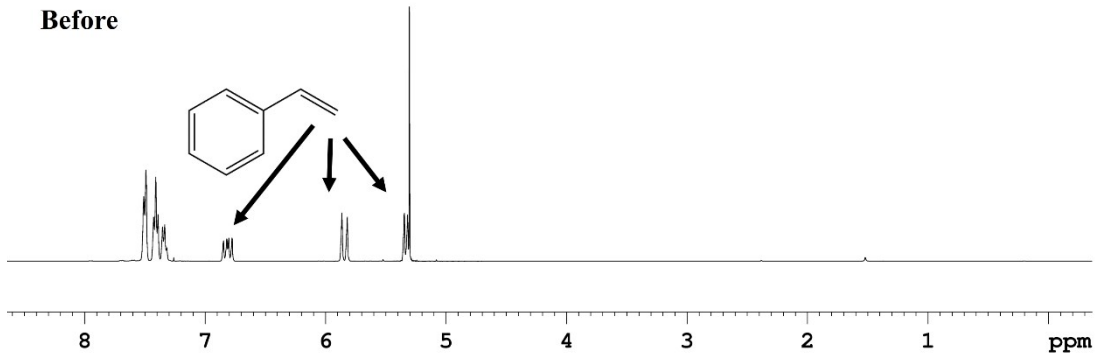


Table 2 entry 2

Table 2 entry 2



Before



Time: 3.08 3.30 3.51 3.72 3.93 4.14 4.35 4.57 4.78 4.99 5.20 5.42 5.62 5.84 6.05 6.26 6.47 6.69 6.90 7.11 7.32 7.53

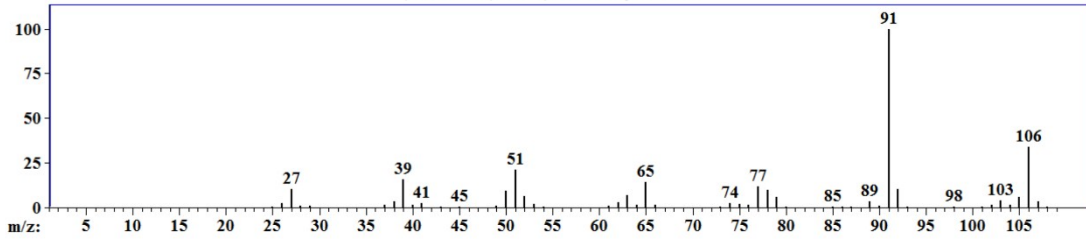
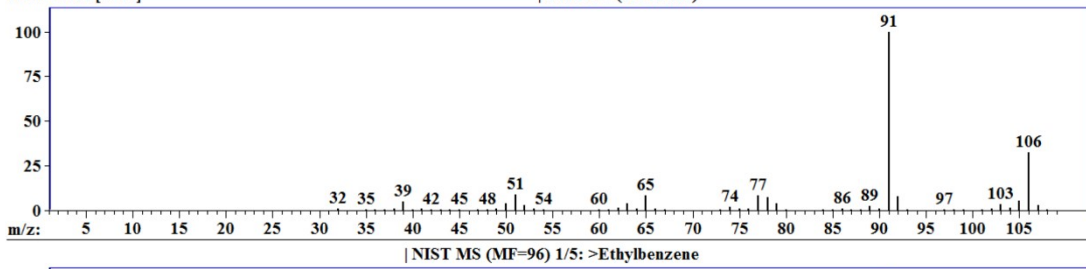


Table 2 entry 3

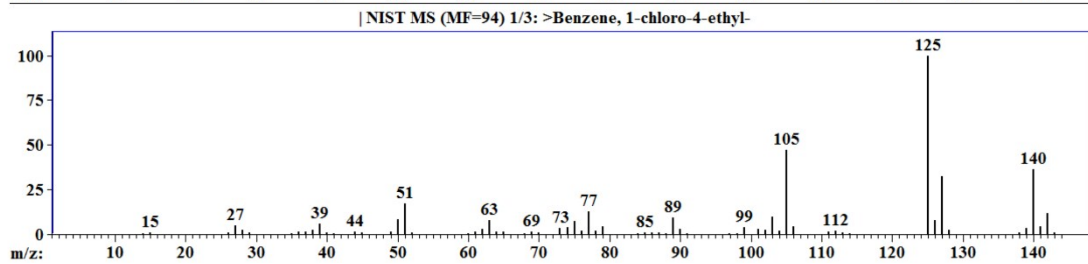
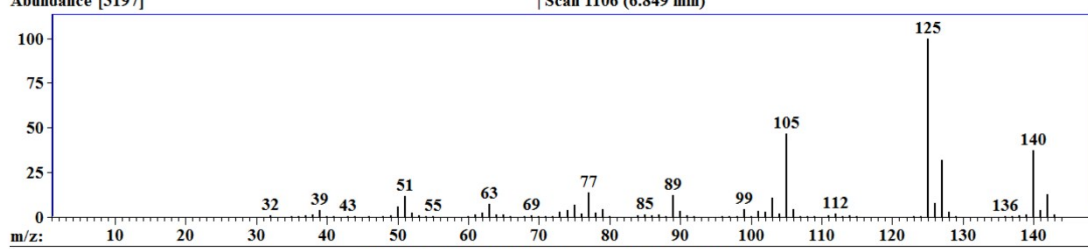
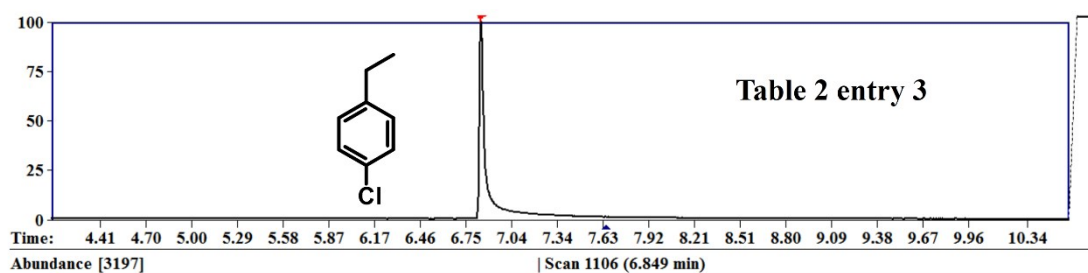
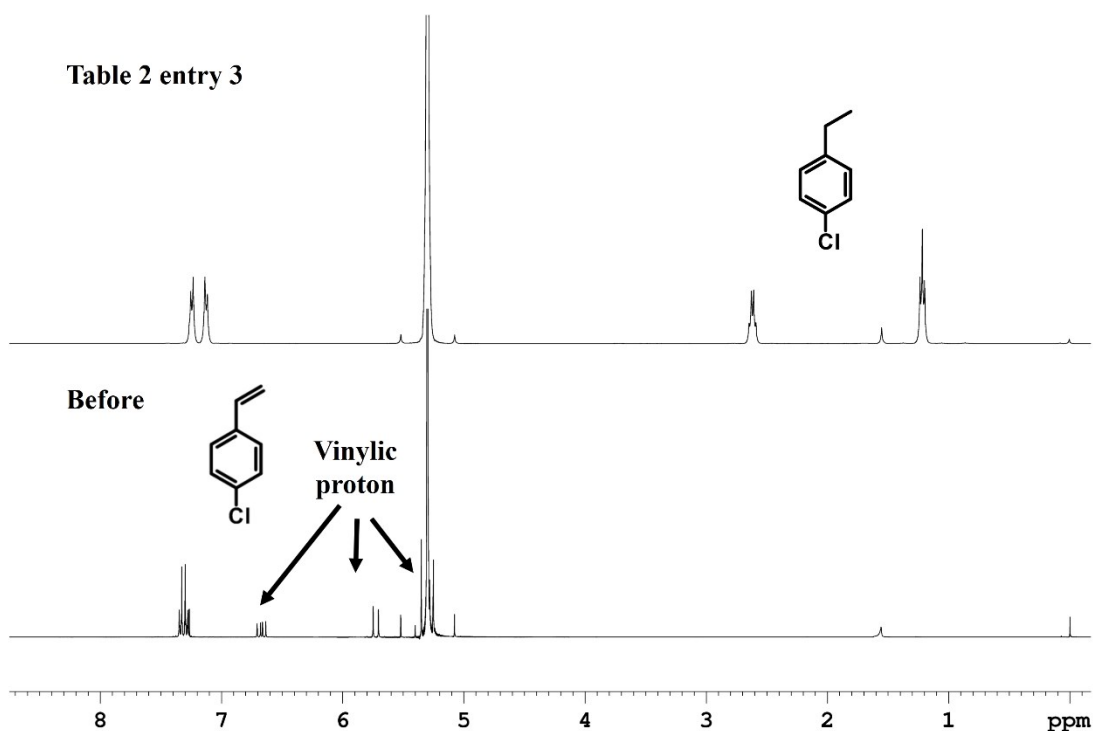


Table 2 entry 4

Table 2 entry 4

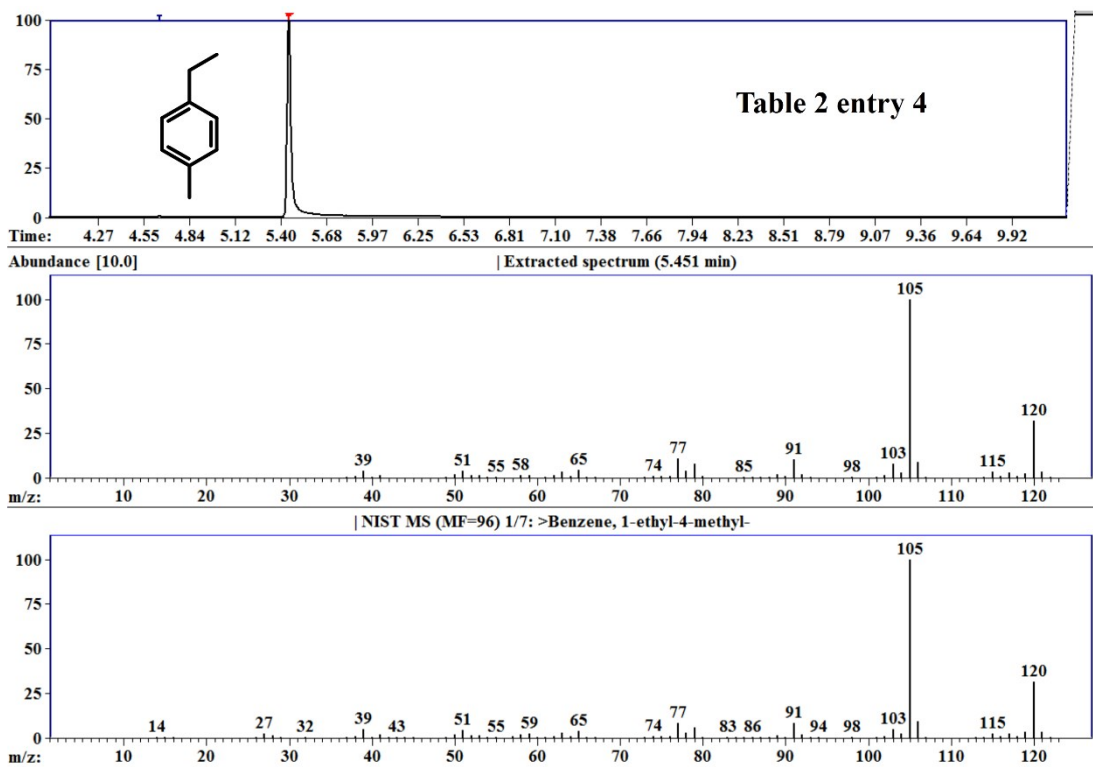
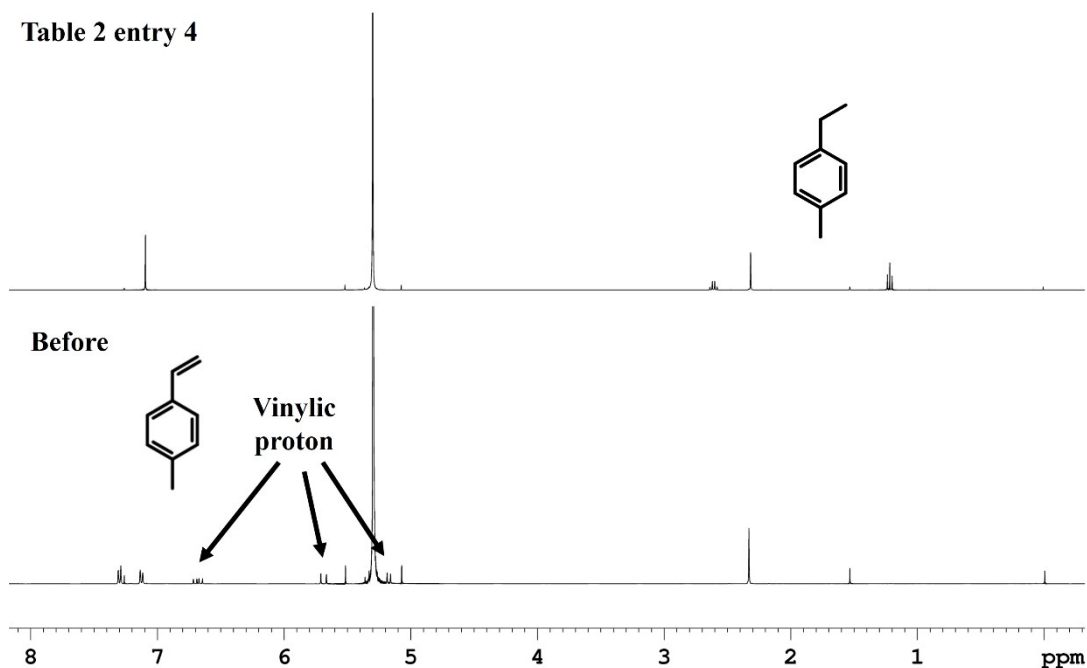
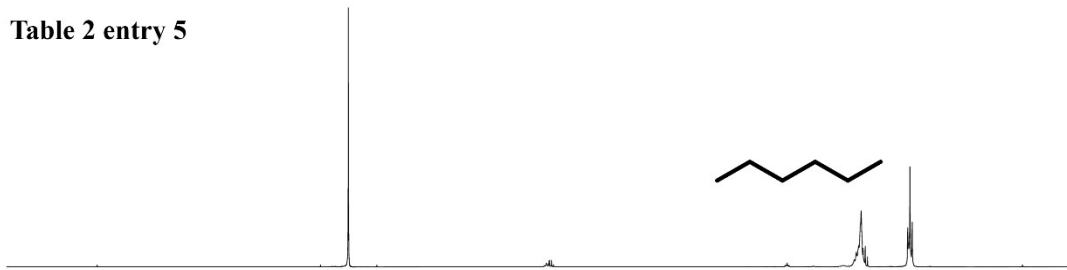


Table 2 entry 5

Table 2 entry 5



Before

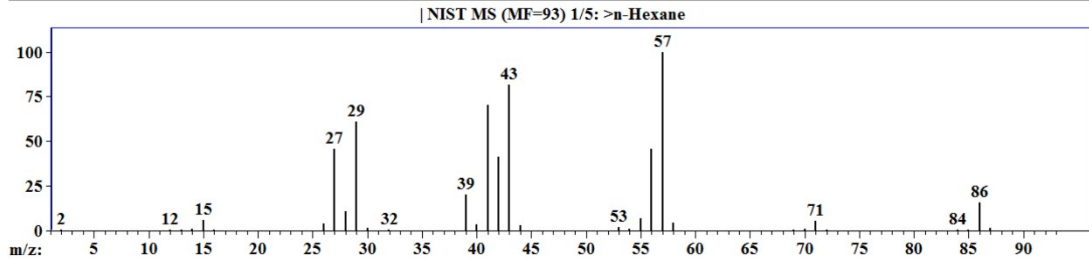
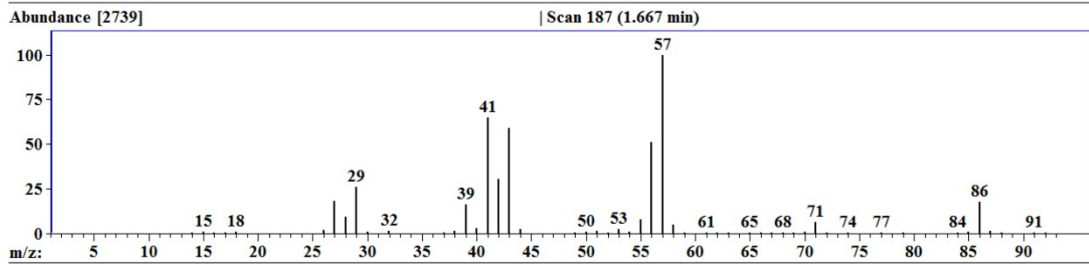
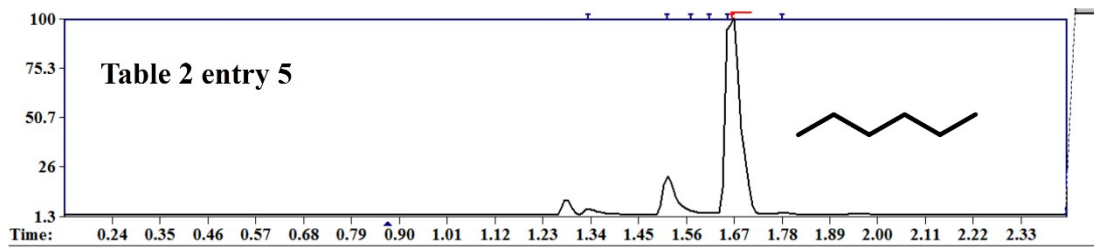
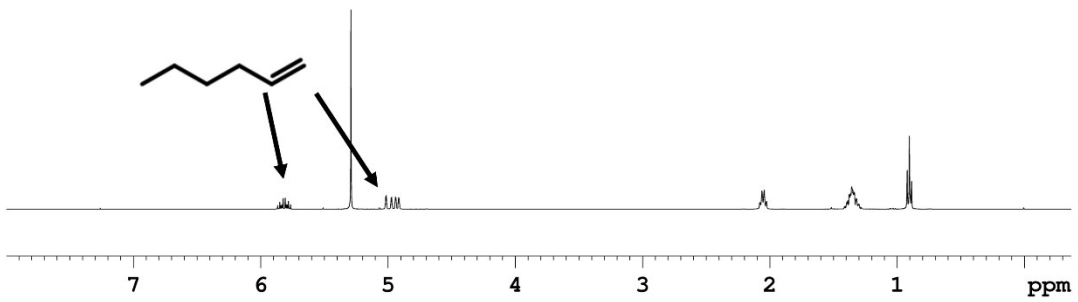
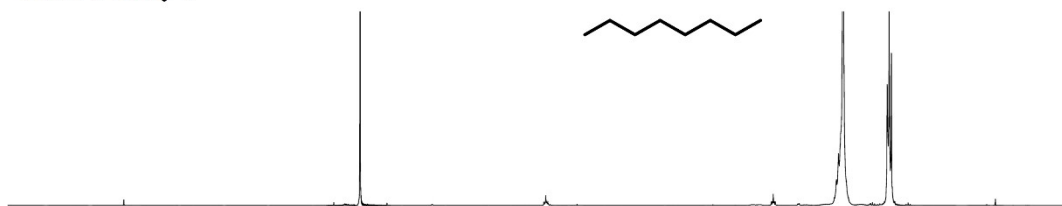


Table 2 entry 6

Table 2 entry 6



Before

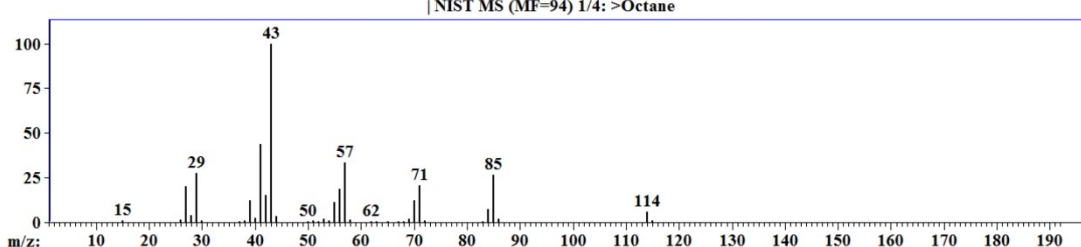
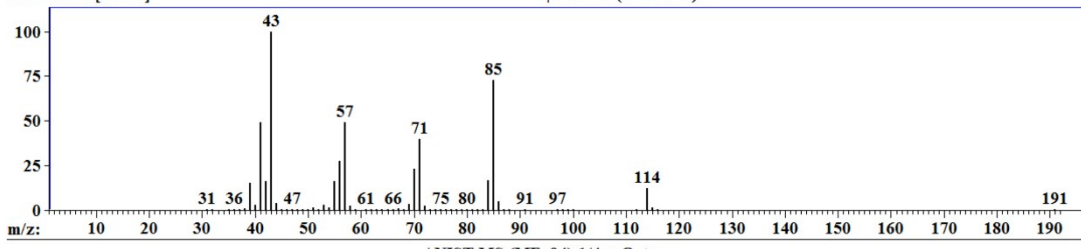
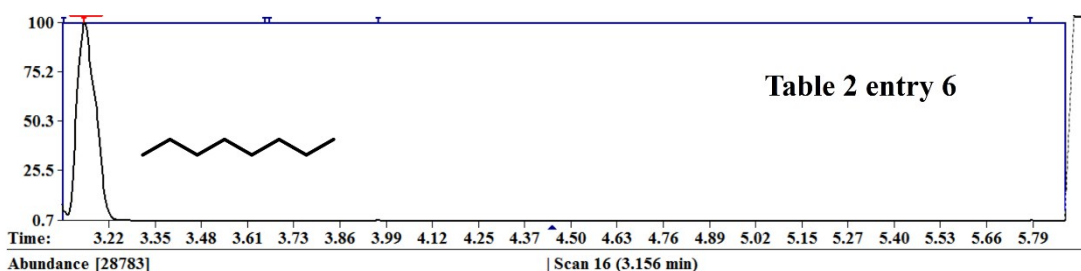
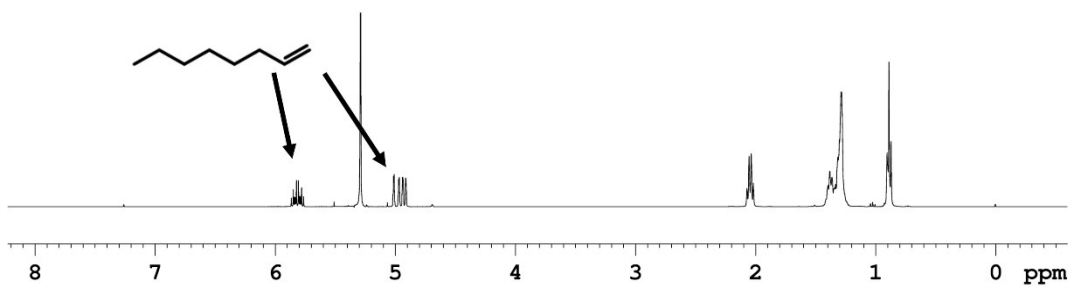
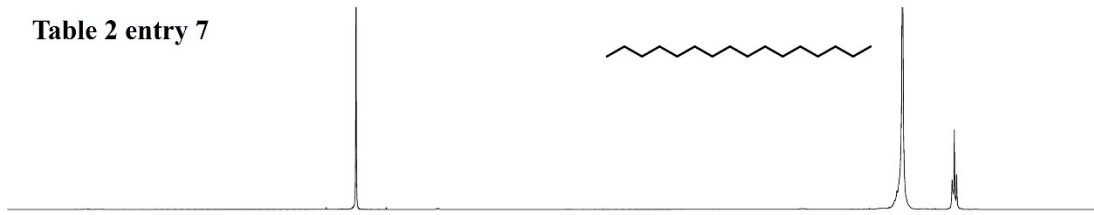


Table 2 entry 7

Table 2 entry 7



Before

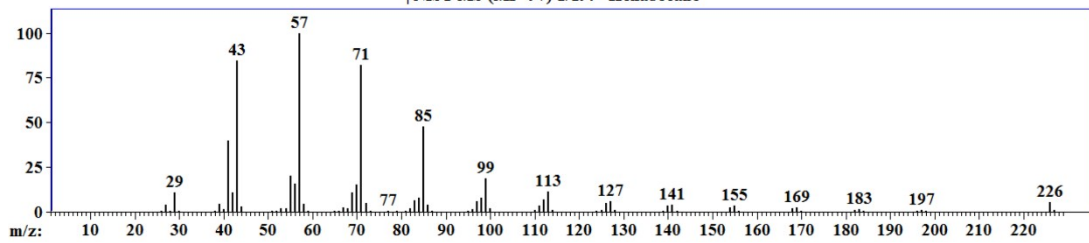
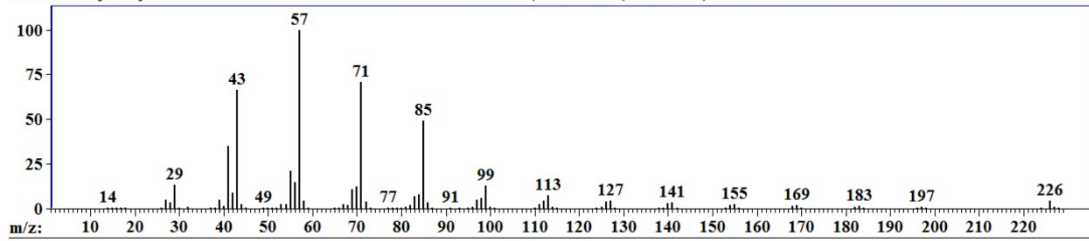
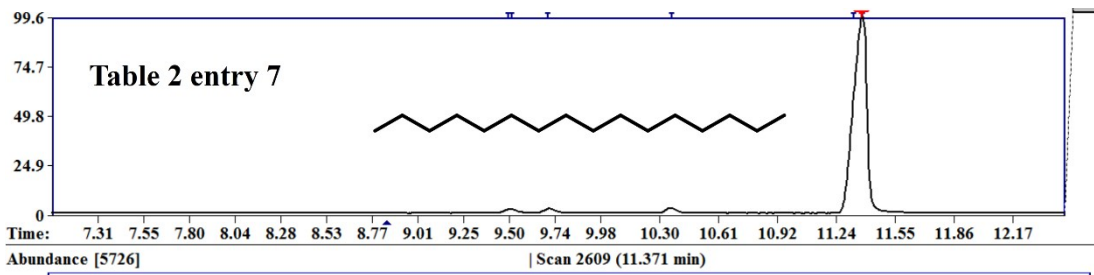
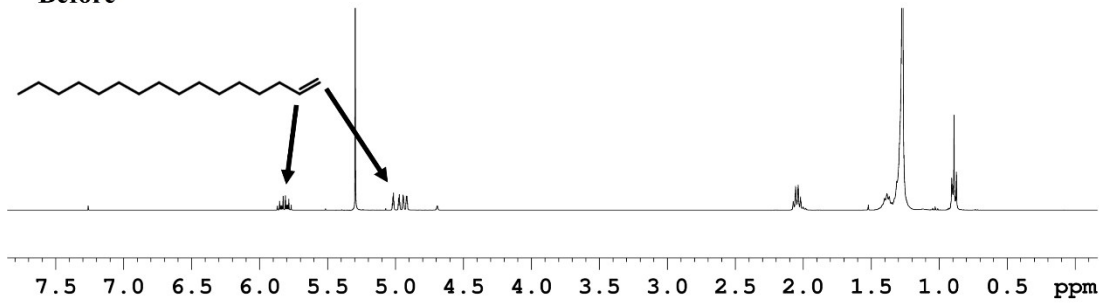


Table 2 entry 8

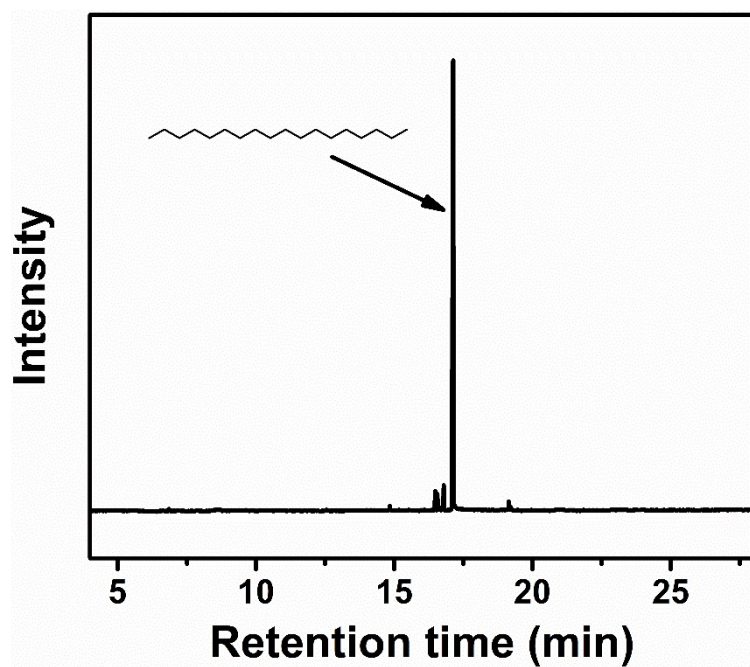
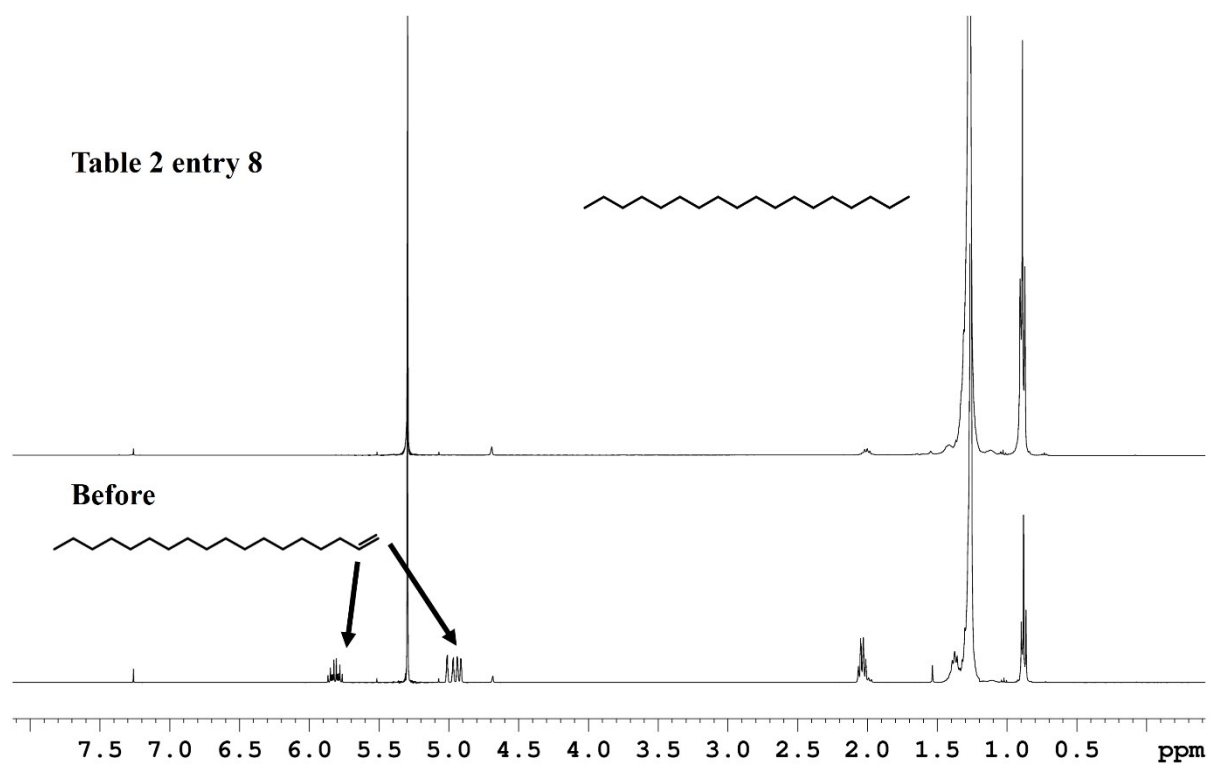


Table 2 entry 9

Table 2 Entry 9

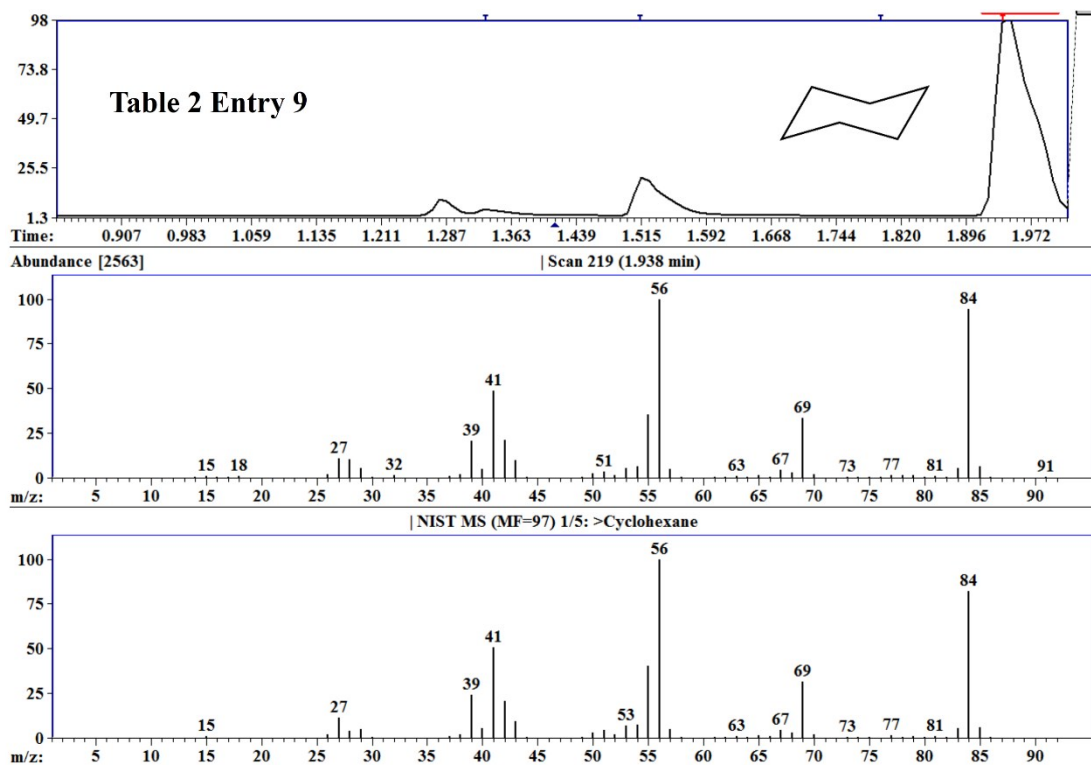
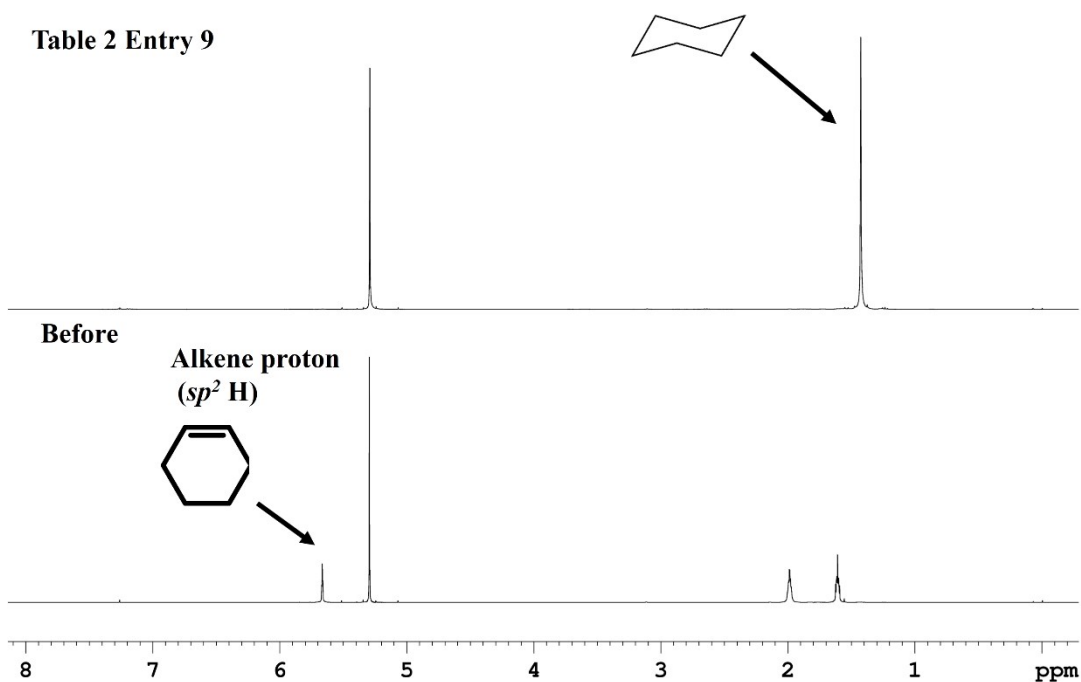


Table 2 entry 10

Table 2 Entry 10

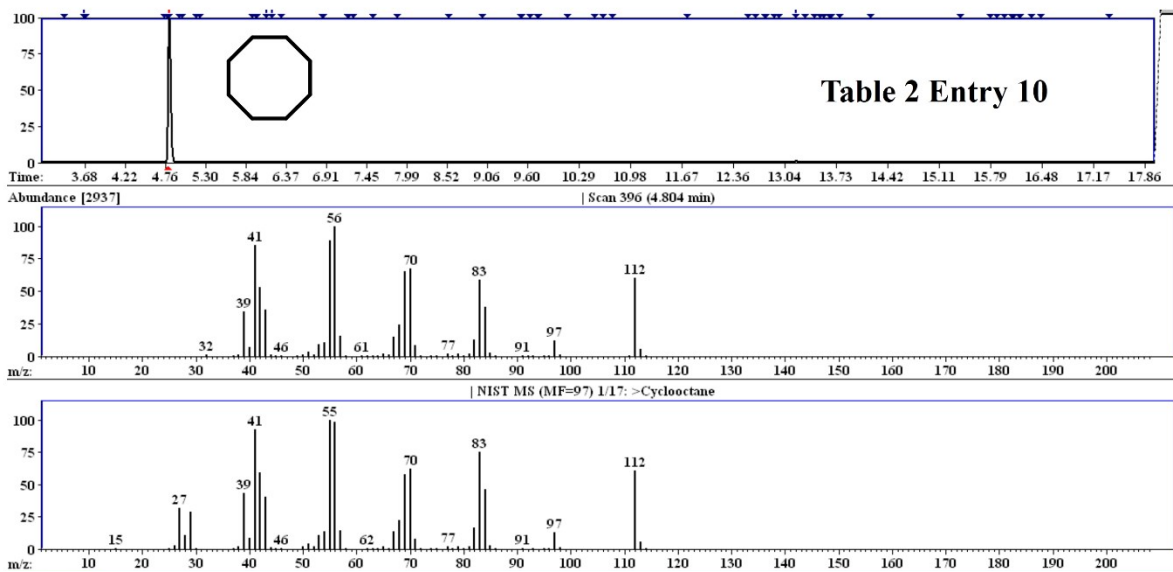
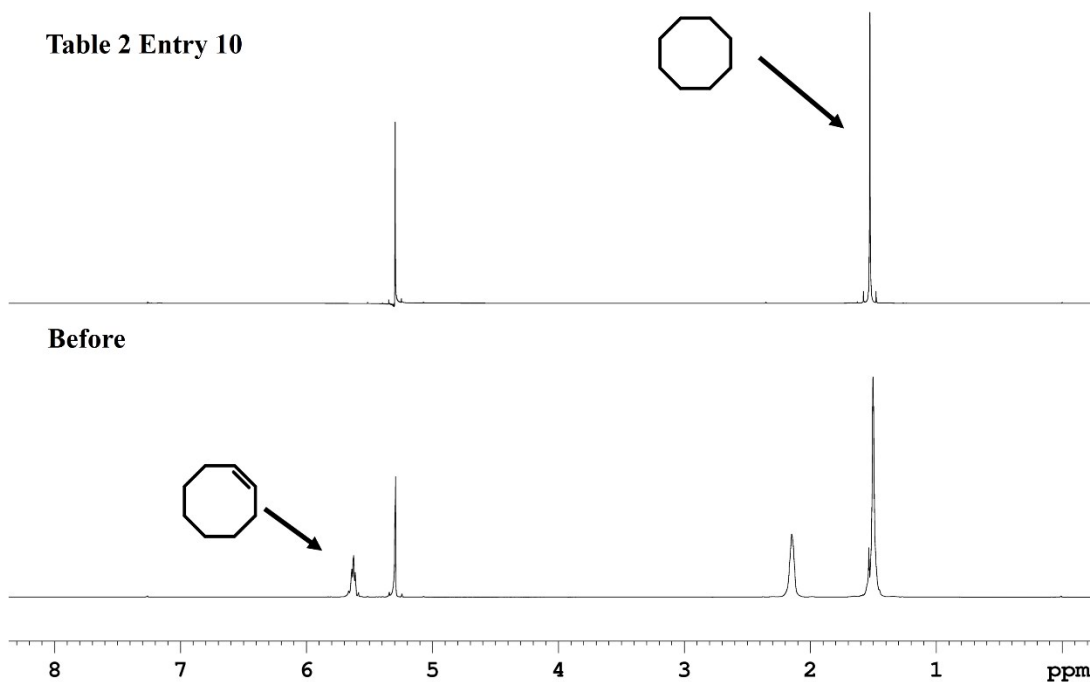
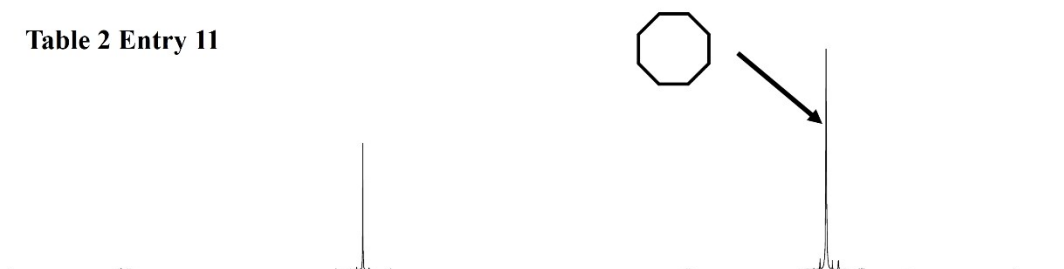


Table 2 entry 11

Table 2 Entry 11



Before

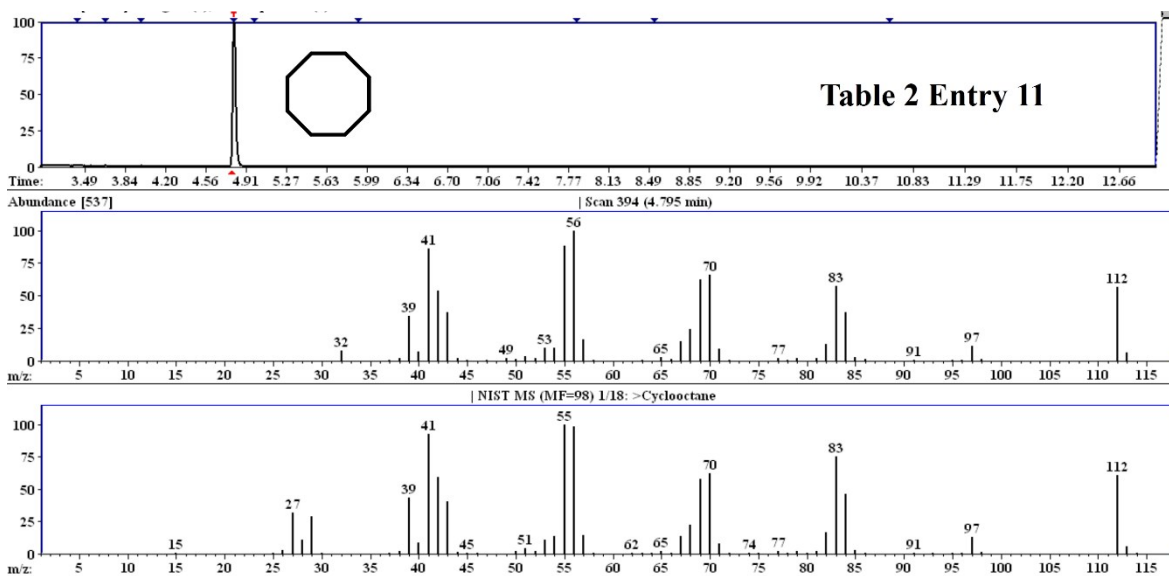
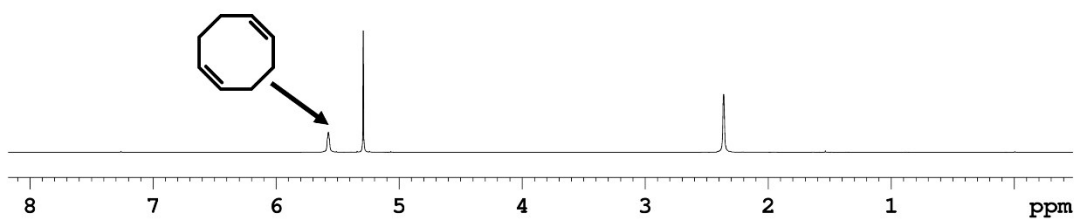


Table 2 entry 12

Table 2 entry 12

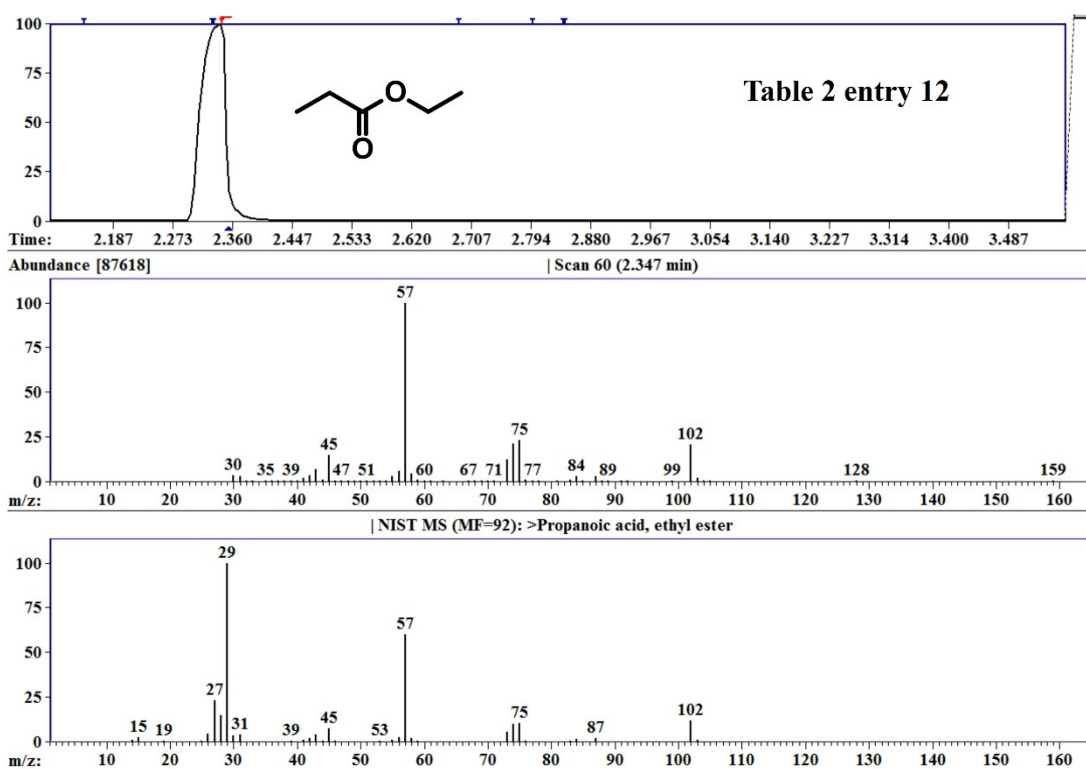
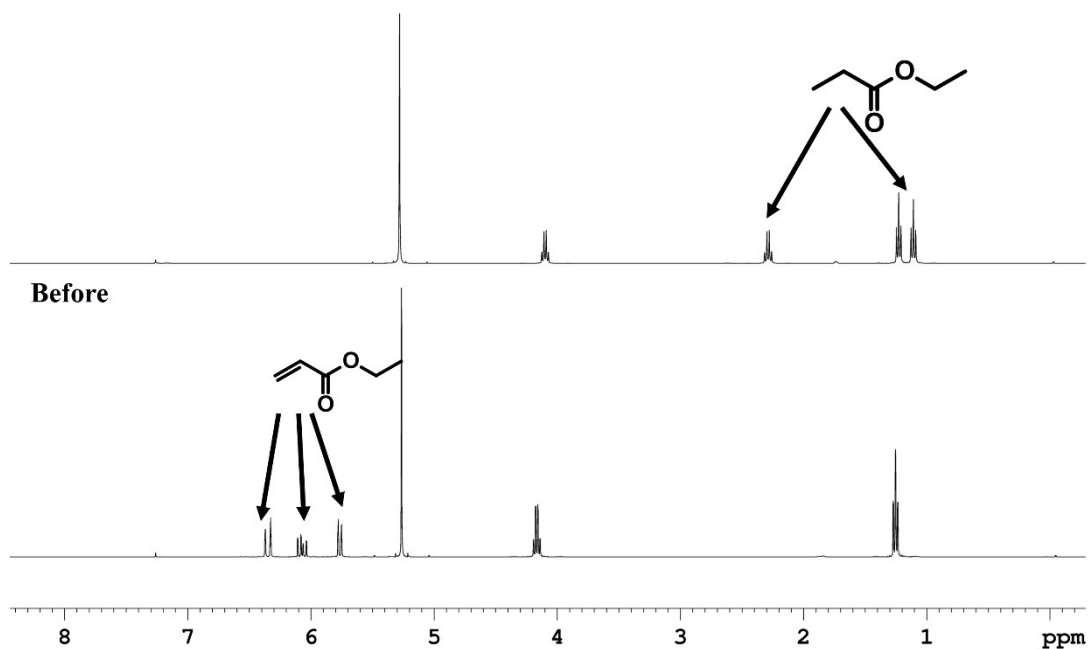


Table 2 entry 13

Table 2 entry 13



Before

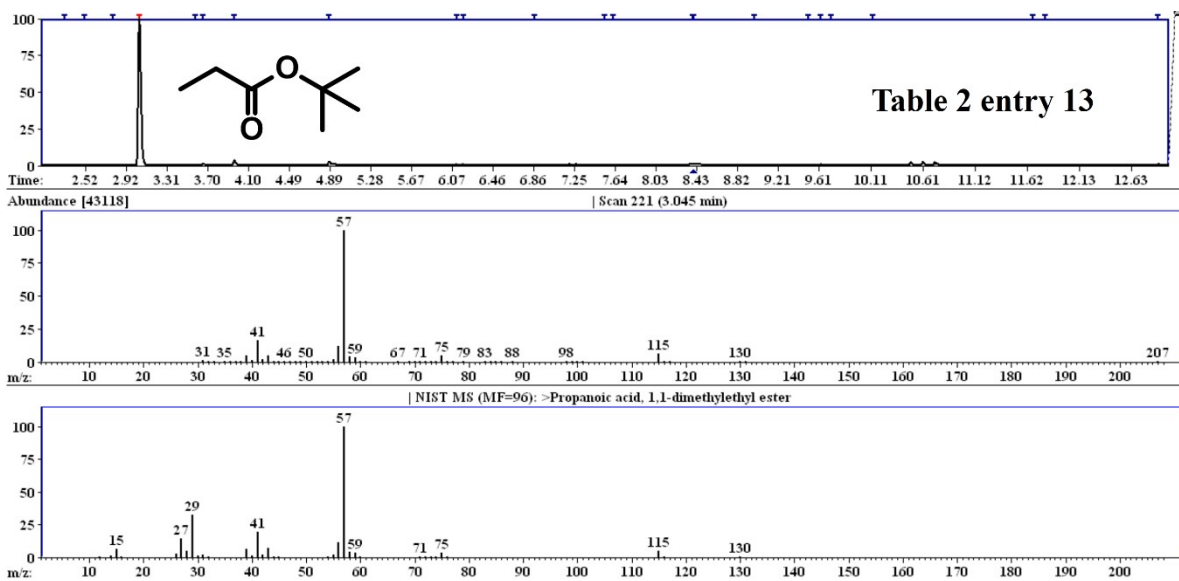
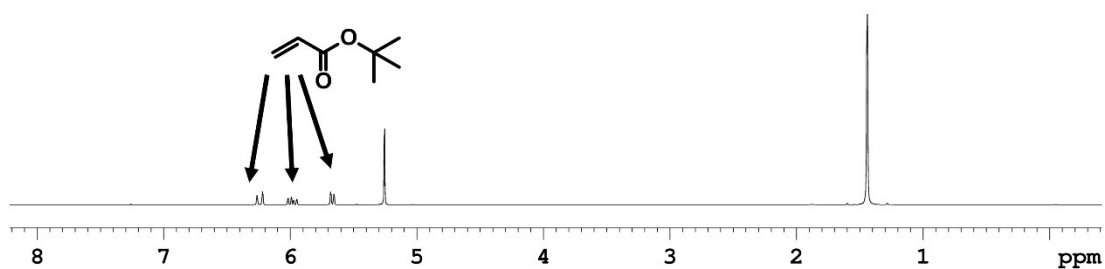


Table 2 entry 14

Table 2 entry 14

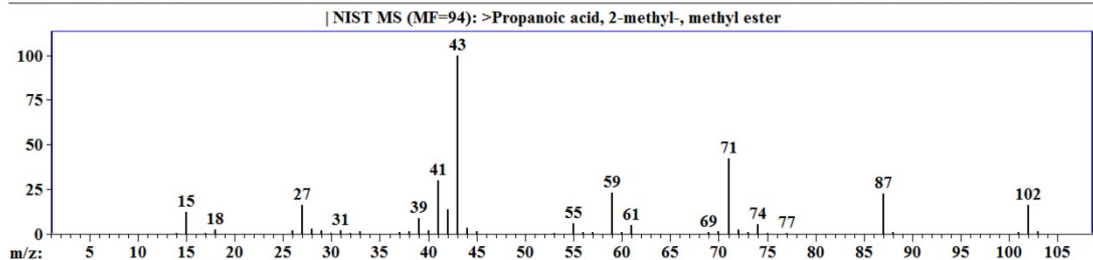
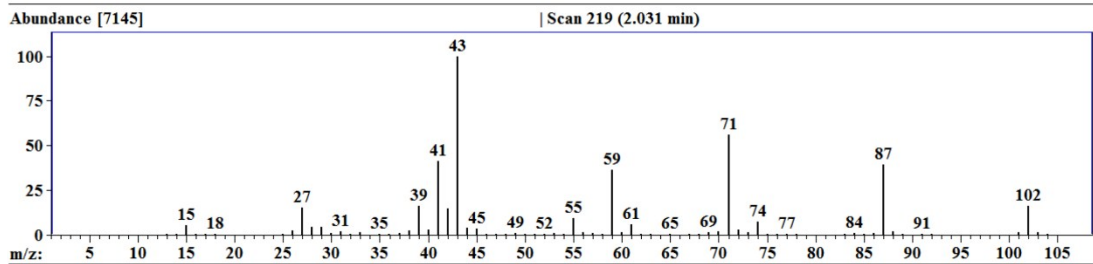
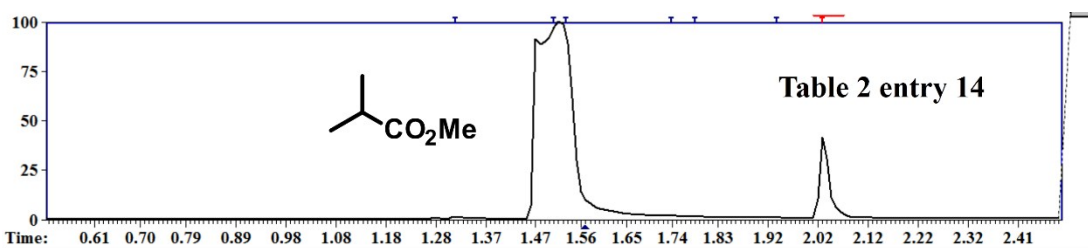
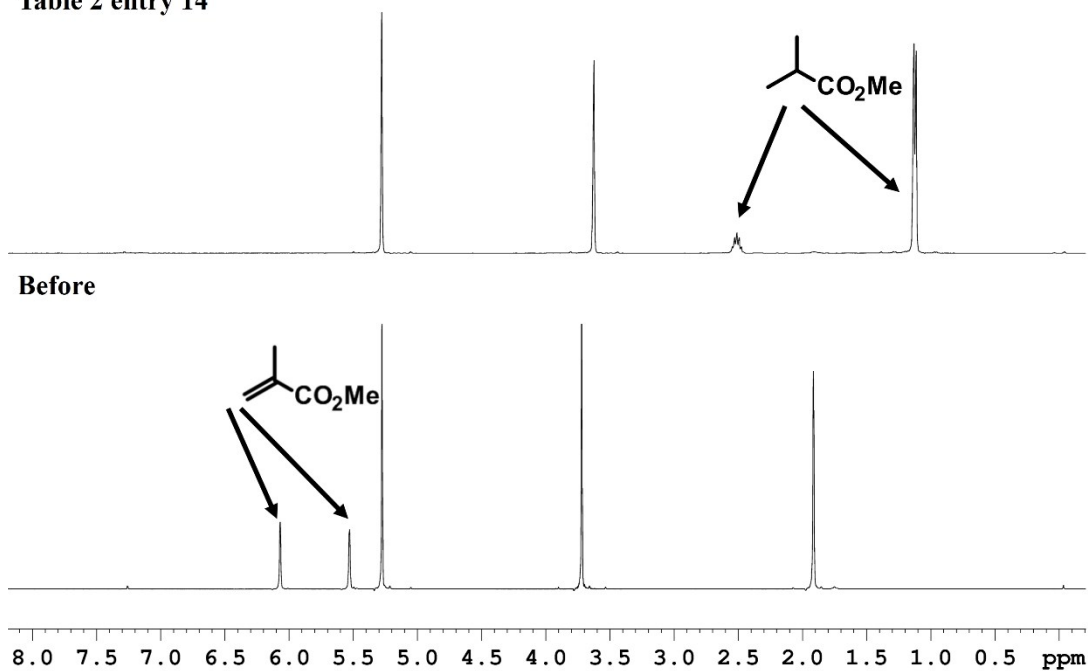
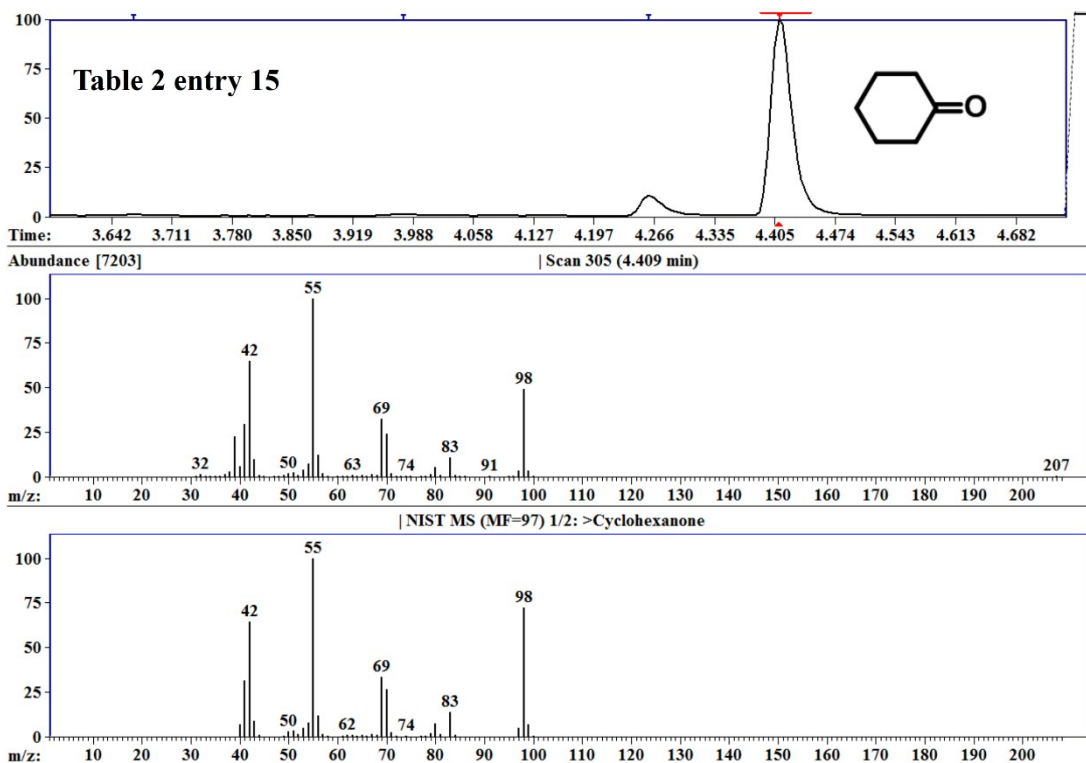
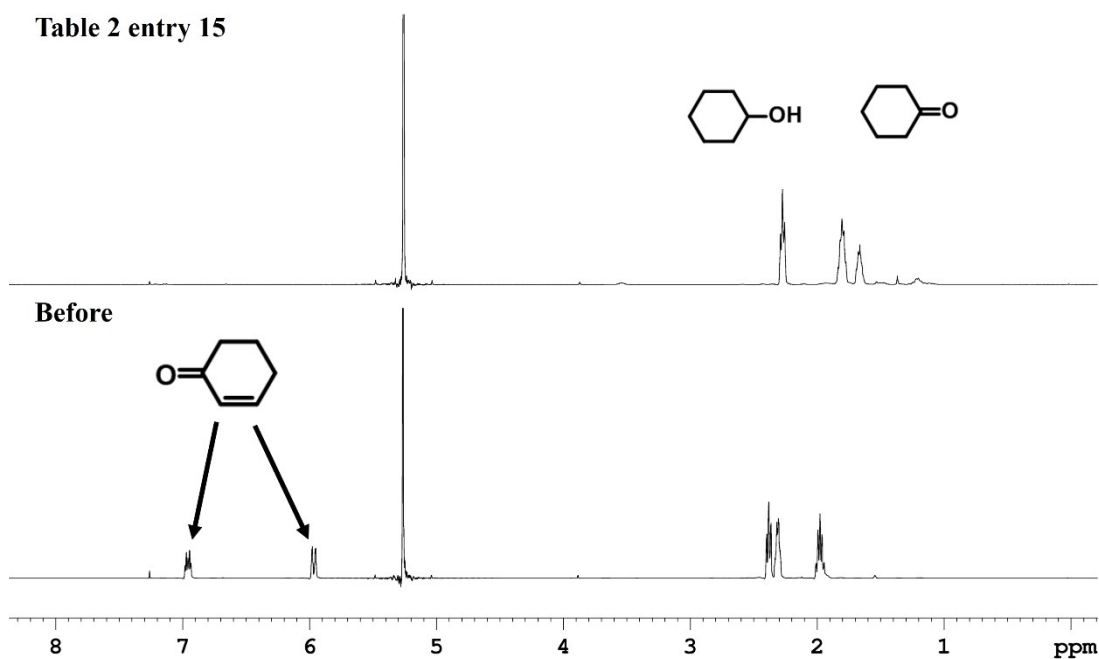


Table 2 entry 15

Table 2 entry 15



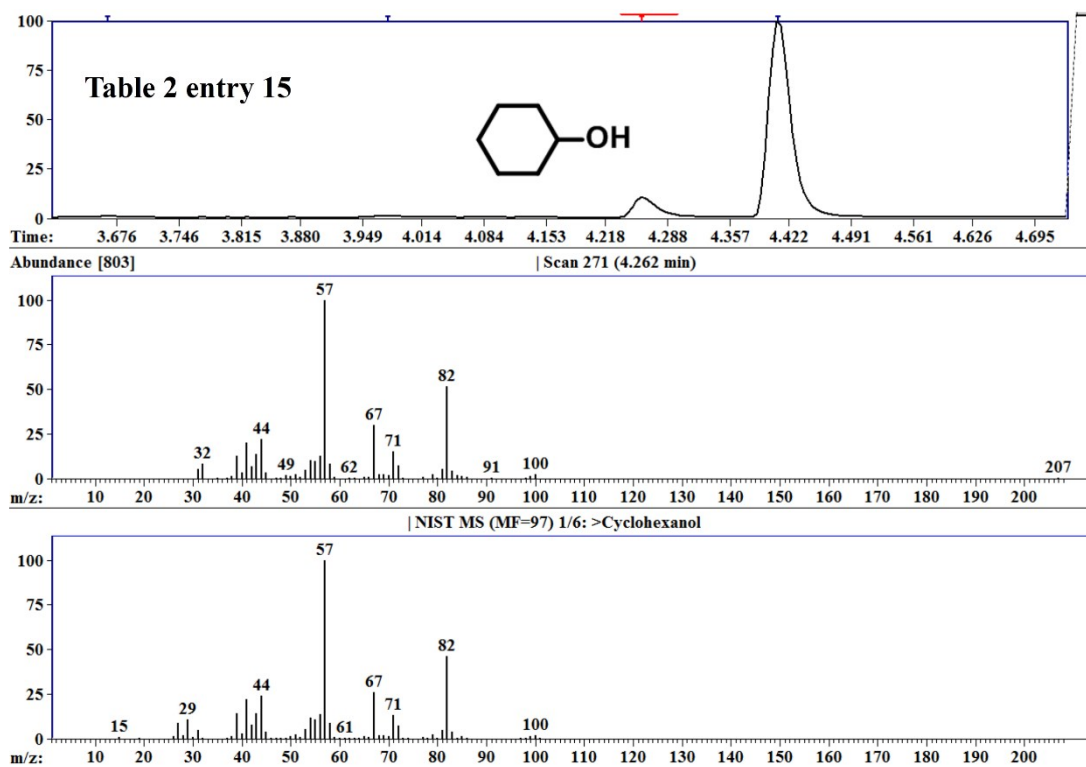


Table 2 entry 16 (Table S2 data) NMR stack plot

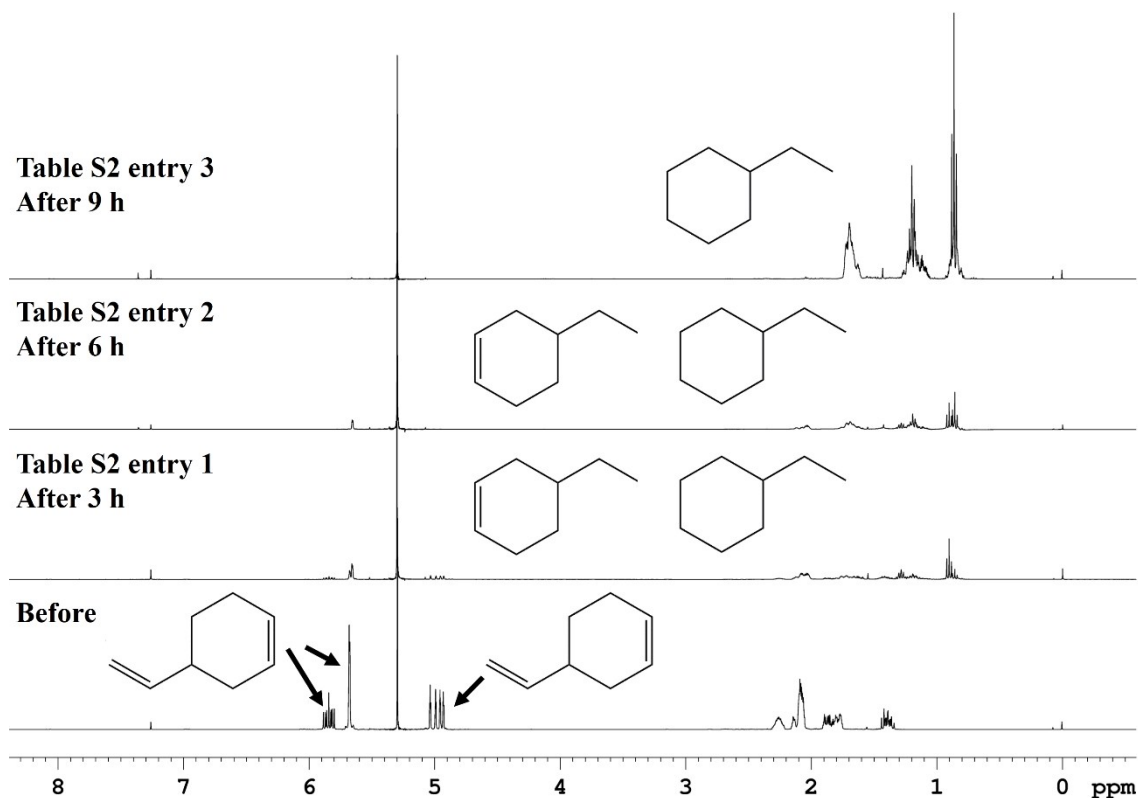


Table 2 entry 16 (Table S2 entry 1) GC-MS plot

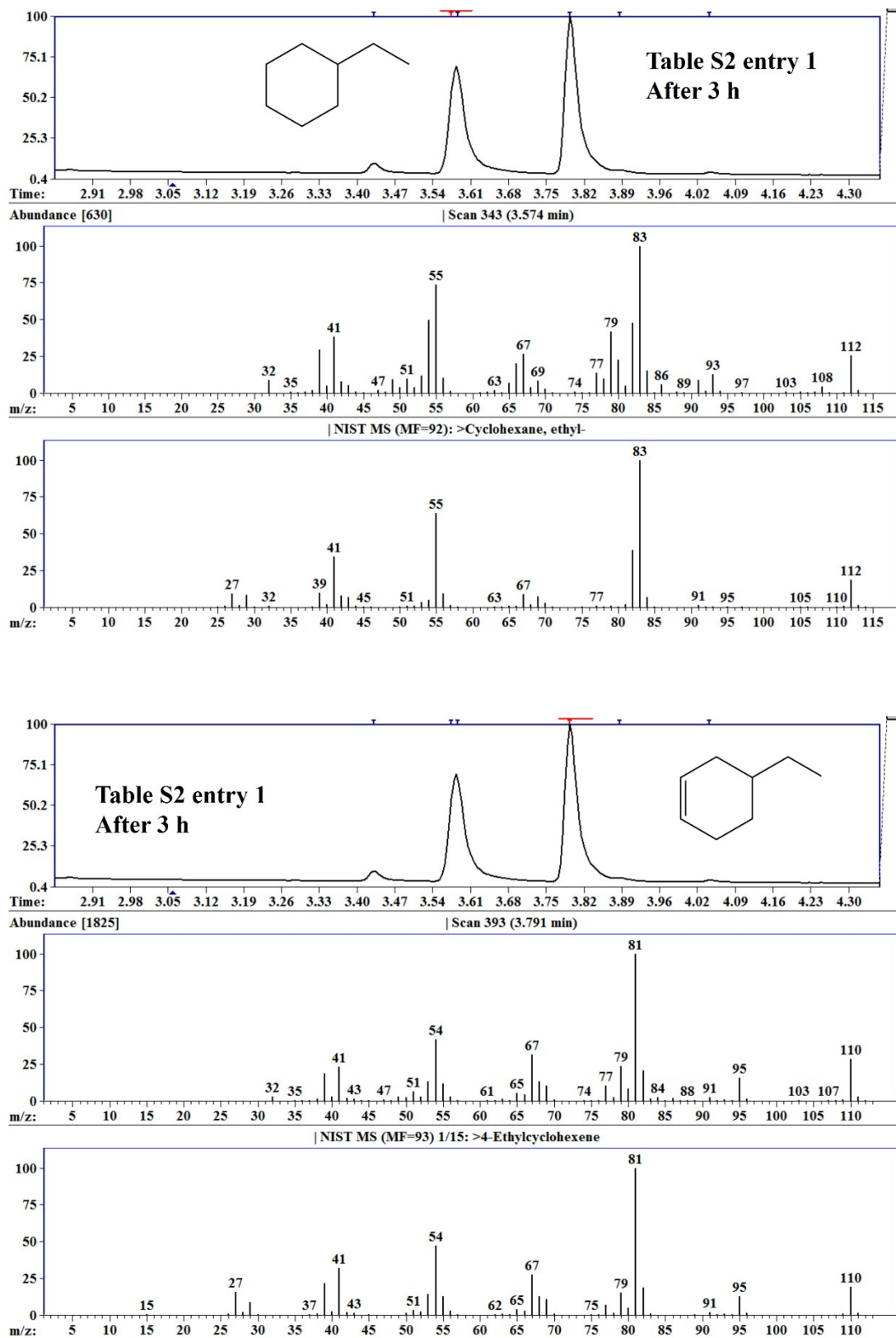


Table 2 entry 16 (Table S2 entry 2) GC-MS plot

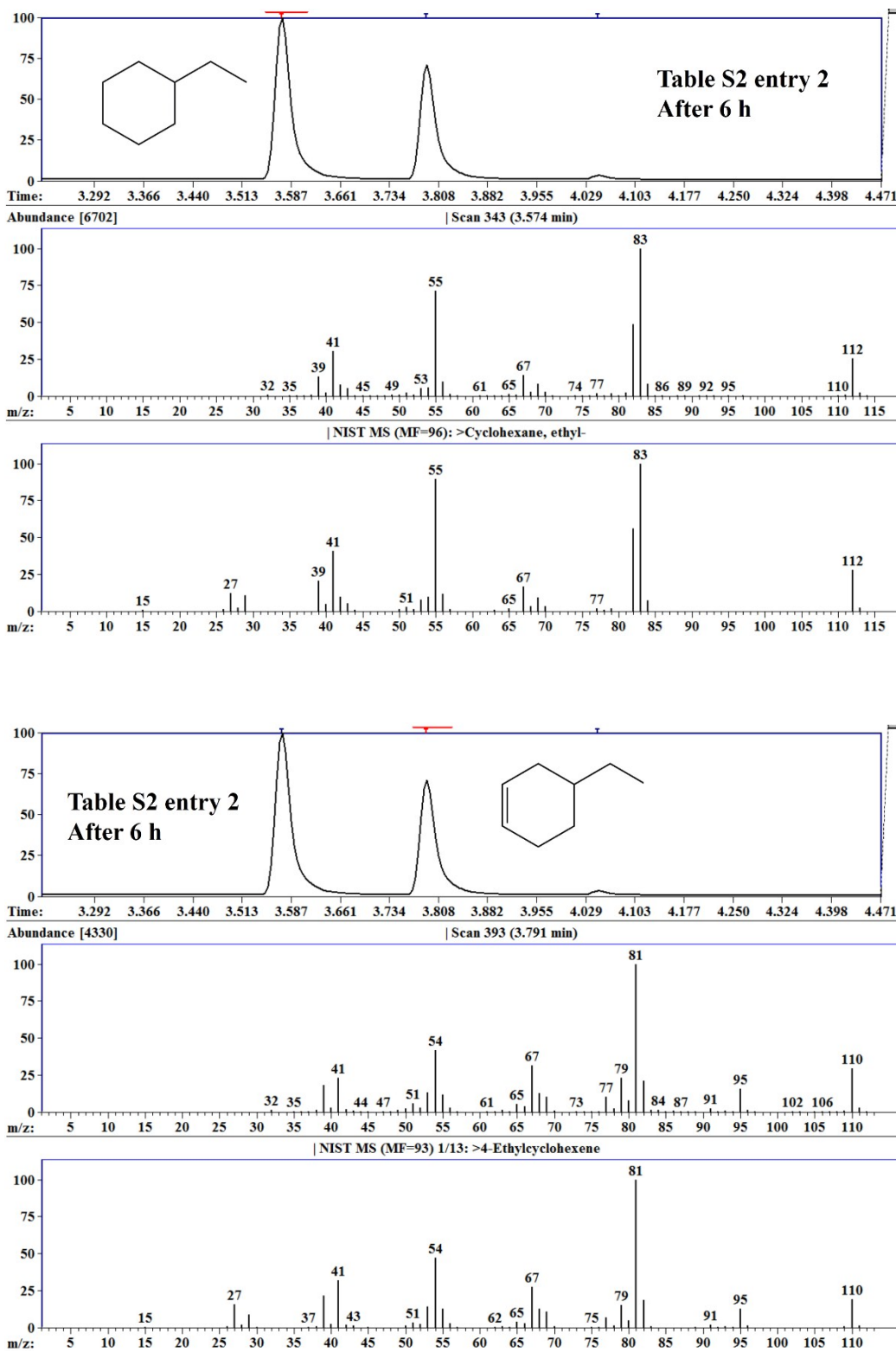


Table 2 entry 16 (Table S2 entry 3) GC-MS plot

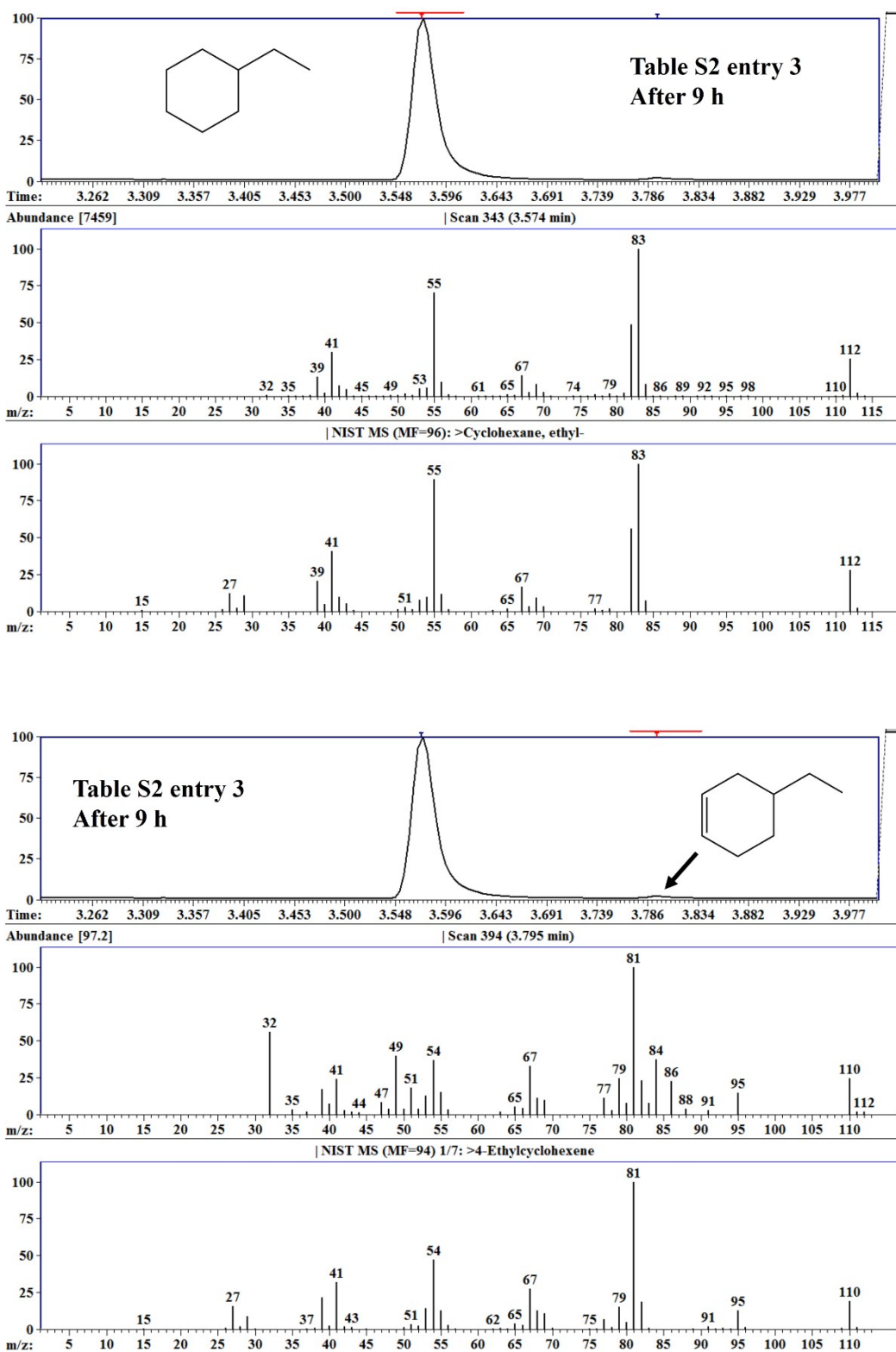


Table 2 entry 17 NMR

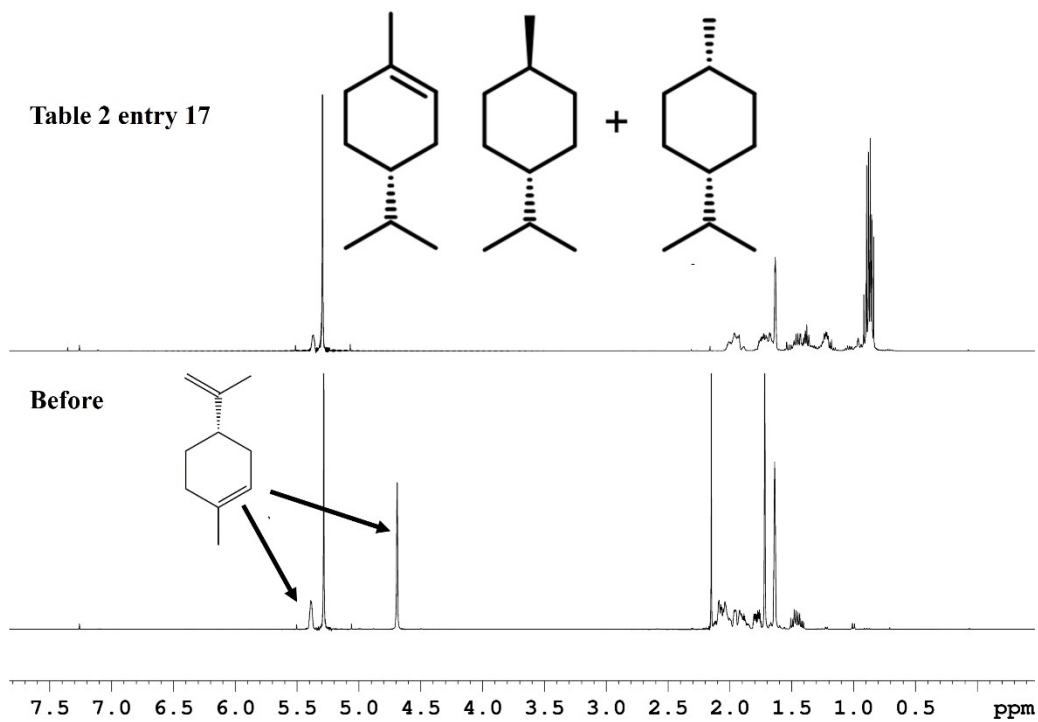
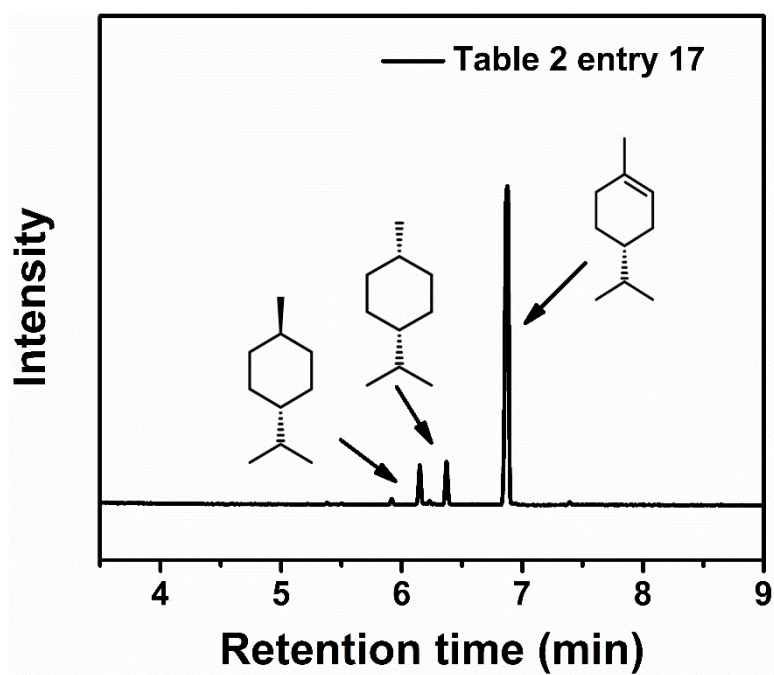


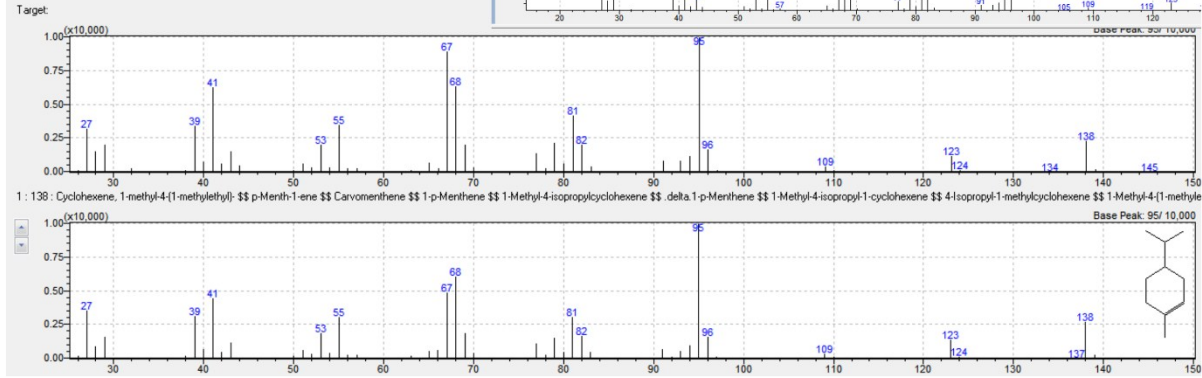
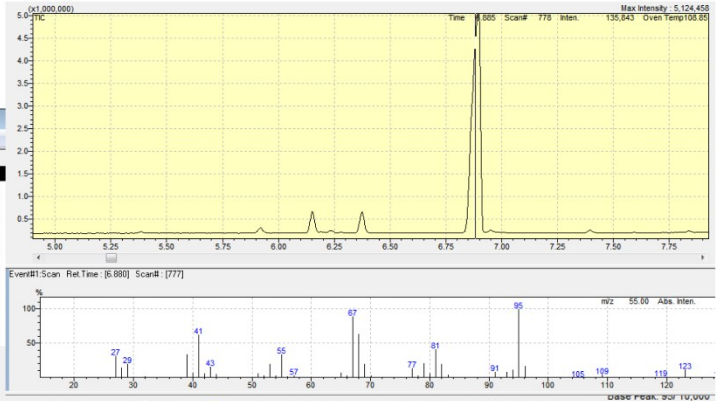
Table 2 entry 17 GC-MS plot



Similarity Search Results

Report View Compound Info Process Help

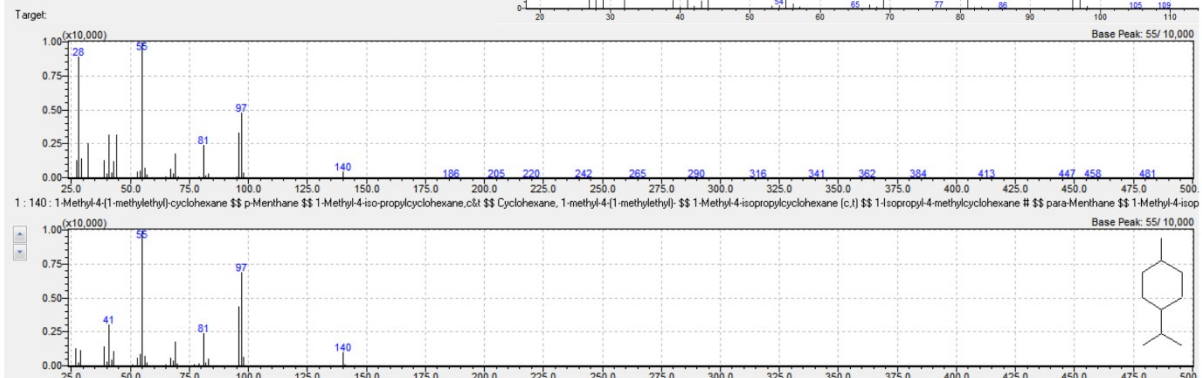
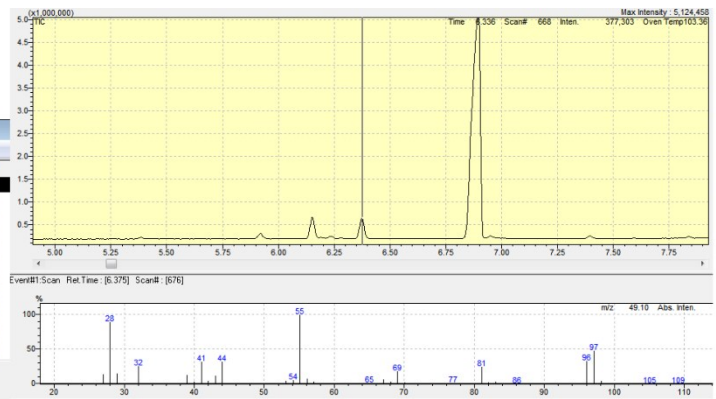
Hit	Similar	Regi	Compound Name	Mol Wt	Formula	Library
1	95	(7)	Cyclohexene, 1-methyl-4-(1-methylethyl)-, SS p-	138	C10H18	NIST11.lb
2	91		Bicyclo[4.1.0]heptane, 3,7,7-trimethyl-, [1S]-1-	138	C10H18	NIST11.lb
3	90		3,5-Octadecene, 2,7-dimethyl-, (Z,Z)-, SS (3Z,5Z)	138	C10H18	NIST11.lb
4	89		Cyclohexene, 1-(2-methylpropyl)-, SS 1-Isobutyl-	138	C10H18	NIST11.lb
5	89		Bicyclo[4.1.0]heptane, 3,7,7-trimethyl-, (1 alpha	138	C10H18	NIST11.lb
6	89		Cyclopentane, 1-methyl-3-(2-methyl-1-propenyl)	138	C10H18	NIST11.lb
7	89		3,5-Octadecene, 2,7-dimethyl-, (E,Z)-, SS (3E,5Z)	138	C10H18	NIST11.lb
8	89		Cyclohexene, 3-methyl-6-(1-methylethyl)-, SS p-	138	C10H18	NIST11.lb
9	89		Bicyclo[4.1.0]heptane, 3,7,7-trimethyl-, [1S]-1-	138	C10H18	NIST11.lb
10	89		1,1'-Bicyclopropyl, 2,2,2',2'-tetramethyl-	138	C10H18	NIST11.lb
11	88		3-Nonyne, SS 3-C9H16, SS	124	C9H16	NIST11.lb
12	88		3-Nonyne, SS 2-C9H16, SS	124	C9H16	NIST11.lb
13	88		Cyclooctane, 1,2-dimethyl-3-(1-methylethenyl)	138	C10H18	NIST11.lb

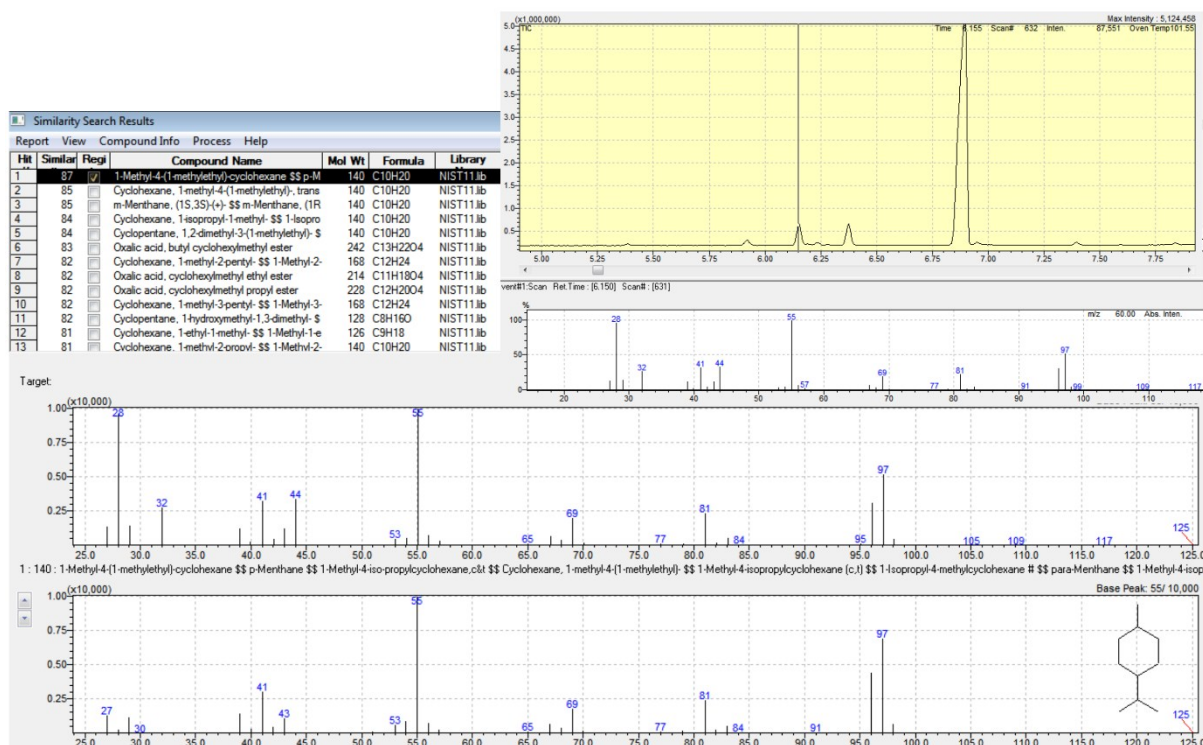


Similarity Search Results

Report View Compound Info Process Help

Hit	Similar	Regi	Compound Name	Mol Wt	Formula	Library
1	88	(7)	1-Methyl-4-(1-methylethyl)-cyclohexane, SS p-M	140	C10H20	NIST11.lb
2	85		Cyclohexane, 1-methyl-4-(1-methylethyl)-, trans	140	C10H20	NIST11.lb
3	85		m-Menthane, (1S,3S)-(+)-, SS m-Menthane, (1R	140	C10H20	NIST11.lb
4	85		Cyclohexane, 1-isopropyl-1-methyl-, SS 1-Isopro	140	C10H20	NIST11.lb
5	83		Oxalic acid, butyl cyclohexylmethyl ester	242	C13H22O4	NIST11.lb
6	83		Cyclopentane, 1,2-dimethyl-3-(1-methylethyl)-, S	140	C10H20	NIST11.lb
7	82		Cyclopentane, 1-hydroxymethyl-1,3-dimethyl-, S	128	C9H18O	NIST11.lb
8	82		Oxalic acid, cyclohexylmethyl ethyl ester	214	C11H18O4	NIST11.lb
9	82		Oxalic acid, cyclohexylmethyl propyl ester	228	C12H20O4	NIST11.lb
10	82		Cyclohexane, 1-methyl-2-ethyl-, SS 1-Methyl-2-	168	C12H24	NIST11.lb
11	82		Cyclohexane, 1-methyl-1-methyl-, SS 1-Methyl-1-e	126	C9H18	NIST11.lb
12	82		Cyclohexane, 1-methyl-3-ethyl-, SS 1-Methyl-3-	168	C12H24	NIST11.lb
13	82		Cyclohexane, 1-ethyl-4-methyl-, cis-, SS cis-1-Et	126	C9H18	NIST11.lb





Gas chromatogram shows three peaks which correspond to the diastereomers of *p*-menthane (*cis* and *trans*) and 1-*p*-menthene. From the retention time and mass spectroscopic investigation the presence of *cis* and *trans* diastereomers could be ascertained. The stereochemistry of 1-*p*-menthene was established using specific rotation measurement. The specific rotation value for the starting material (*R*-limonene, 97%) is $[\alpha]_D^{22} +113.4$ (*c* 2.0, CH₂Cl₂). Whereas, the specific rotation of product is $[\alpha]_D^{22} +101.9$ (*c* 2.0, CH₂Cl₂), which matches with that of the *R* isomer of 1-*p*-menthene (83.5 % calculated from GC). Thus, there is retention of stereochemistry of the chiral center.

Table 2 entry 18 NMR stack plot

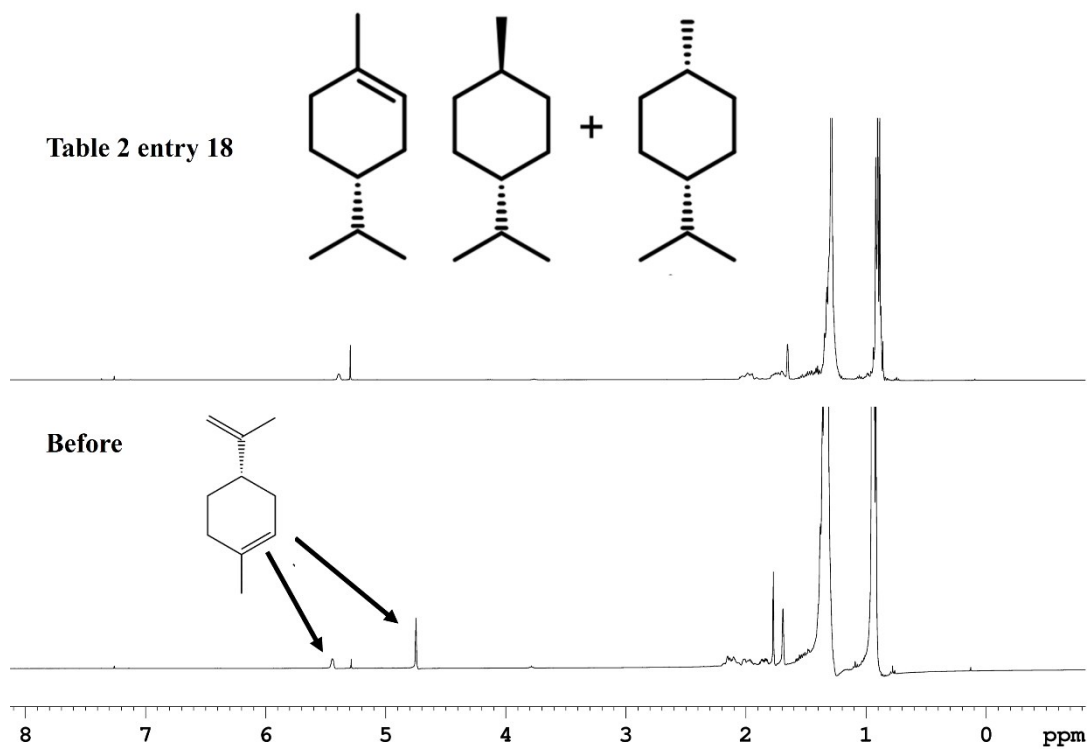
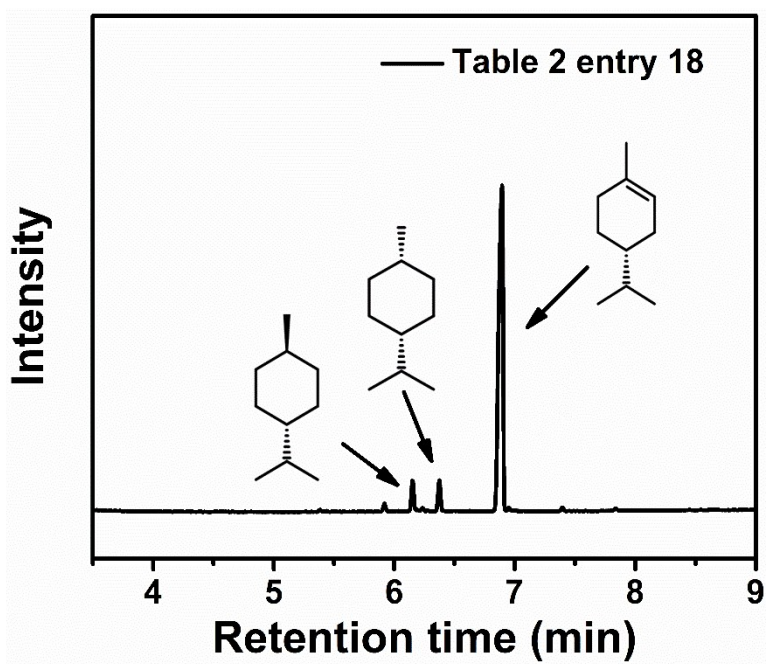
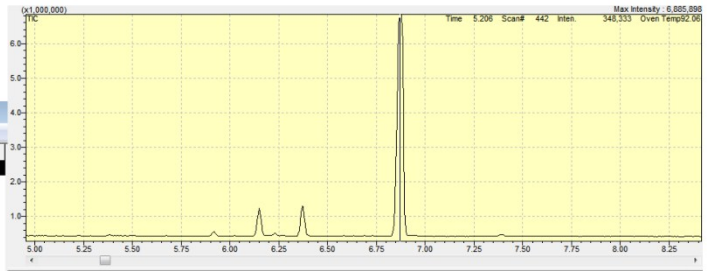


Table 2 entry 18 GC-MS plot

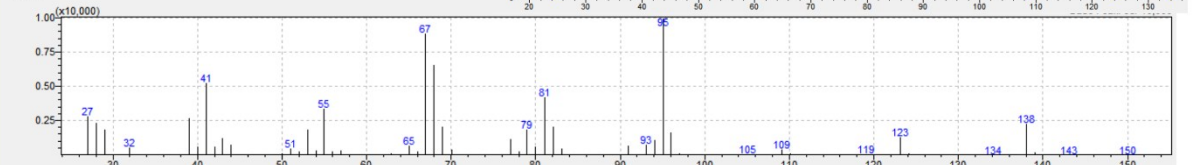


Similarity Search Results

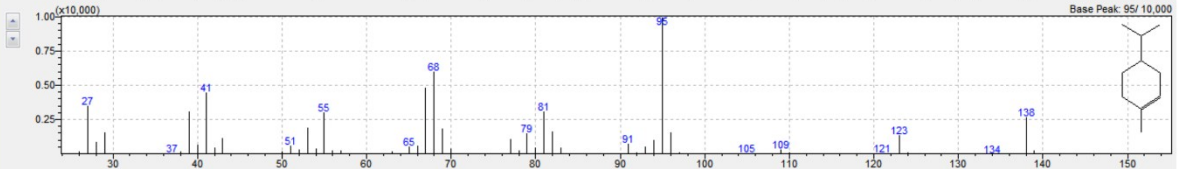
Hit	Similar	Regi	Compound Name	Mol Wt	Formula	Library
1	84	(✓)	Cyclohexene, 1-methyl-4-(1-methylethyl)-, (1R,2S)-	138	C10H18	NIST1111b
2	89		Bicyclo[4.1.0]heptane, 3,7,7-trimethyl-, (1S,2S)-	138	C10H18	NIST1111b
3	89		Bicyclo[4.1.0]heptane, 3,7,7-trimethyl-, (1S,1R)-	138	C10H18	NIST1111b
4	89		Bicyclo[4.1.0]heptane, 3,7,7-trimethyl-, (1R,2S)-	138	C10H18	NIST1111b
5	89		3,5-Octadecene, 2,7-dimethyl-, (Z,Z)-, (3Z,5Z)	138	C10H18	NIST1111b
6	88		Cyclohexene, 1-(2-methylpropyl)-, (1R)-	138	C10H18	NIST1111b
7	88		Cyclohexene, 3-methyl-6-(1-methylethyl)-, (1R,2S)-	138	C10H18	NIST1111b
8	88		Cyclopentane, 1-methyl-3-(2-methyl-1-propenyl)-	138	C10H18	NIST1111b
9	88		3-Norbornene, 2,7-dimethyl-, (E,Z)-, (3E,5Z)	124	C9H16	NIST1111b
10	88		3,5-Octadecene, 2,7-dimethyl-, (E,Z)-, (3E,5Z)	138	C10H18	NIST1111b
11	87		1,1'-Bicyclopropyl, 2,2,2',2'-tetramethyl-, (1R,1'R)-	138	C10H18	NIST1111b
12	87		Cyclopentane, 1,2-dimethyl-3-(1-methylethyl)-	138	C10H18	NIST1111b
13	87		Cyclohexene, 1-methyl-4-(1-methylethyl)-, (1R,2S)-	138	C10H18	NIST1111b



Target:

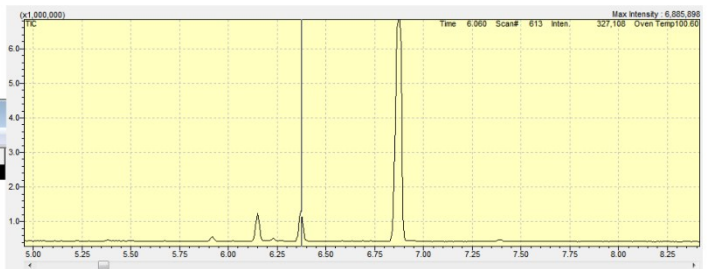


1 : 138: Cyclohexene, 1-methyl-4-(1-methylethyl)-, (1R,2S)-; p-Menth-1-ene; Camphene; 1-p-Menthene; 1-Methyl-4-isopropylcyclohexene; delta-1-p-Menthene; 1-Methyl-4-isopropyl-1-cyclohexene; 4-isopropyl-1-methylcyclohexene; 1-Methyl-4-(1-methyl-2-propenyl)cyclohexene

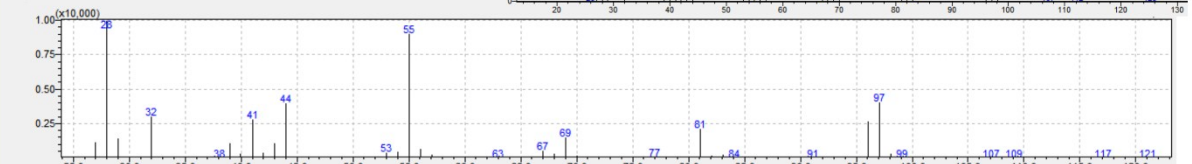


Similarity Search Results

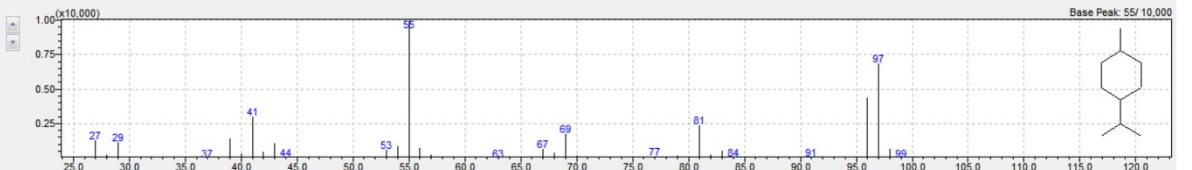
Hit	Similar	Regi	Compound Name	Mol Wt	Formula	Library
1	84	(✓)	1-Methyl-4-(1-methylethyl)cyclohexane, (1R,2S)-	140	C10H20	NIST1111b
2	83		Cyclohexane, 1-methyl-4-(1-methylethyl)-, trans-	140	C10H20	NIST1111b
3	83		m-Menthane, (1S,3S)-, (+)-, (1R)	140	C10H20	NIST1111b
4	82		Cyclohexane, 1-isopropyl-1-methyl-, (1R)-	140	C10H20	NIST1111b
5	82		Oxalic acid, butyl cyclohexylmethyl ester	242	C13H22O4	NIST1111b
6	81		Cyclopentane, 1,2-dimethyl-3-(1-methylethyl)-, (1R,2S)-	140	C10H20	NIST1111b
7	81		Oxalic acid, cyclohexylmethyl ethyl ester	214	C11H18O4	NIST1111b
8	80		Cyclopentane, 1-hydroxymethyl-1,3-dimethyl-, (1R,2S)-	128	C8H16O	NIST1111b
9	80		Cyclohexane, 1-ethyl-1-methyl-, (1R)-	126	C9H18	NIST1111b
10	80		Cyclohexane, 1-methyl-3-propyl-, (1R)-	168	C12H24	NIST1111b
11	80		Cyclohexane, 1-ethyl-2-methyl-, (1R)-	126	C9H18	NIST1111b
12	80		Oxalic acid, cyclohexylmethyl propyl ester	228	C12H20O4	NIST1111b
13	79		Cyclohexane, 1-methyl-2-ethyl-, (1R)-	168	C12H24	NIST1111b



Target:



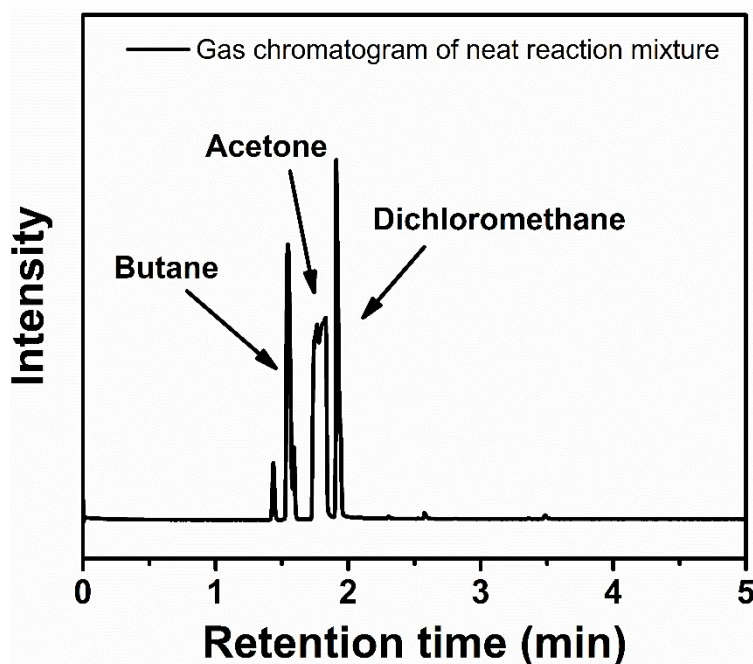
1 : 140: 1-Methyl-4-(1-methylethyl)cyclohexane; p-Menthane; 1-Methyl-4-isopropylcyclohexane, (1R,2S)-; Cyclohexane, 1-methyl-4-(1-methylethyl)-, (1R,2S)-; 1-Methyl-4-isopropylcyclohexane; (1R,2S)-1-isopropyl-4-methylcyclohexane; para-Menthane; 1-Methyl-4-(1-methyl-2-propenyl)cyclohexane





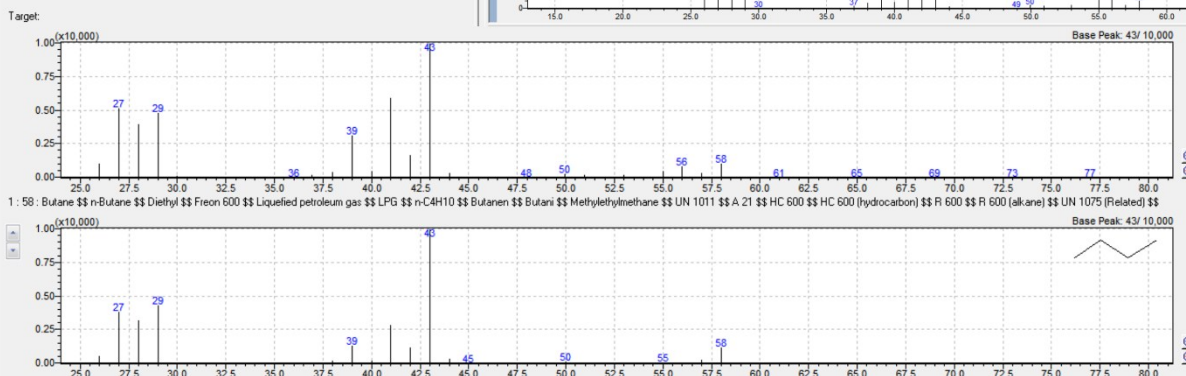
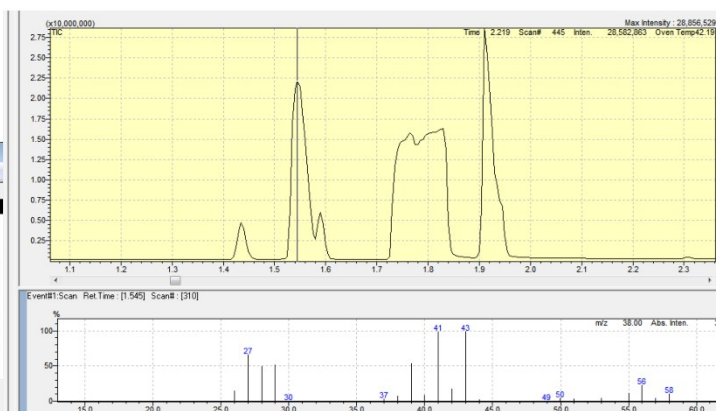
Gas chromatogram shows three peaks, corresponding to the diastereomers of *p*-menthane (*cis* and *trans*) and 1-*p*-menthene. From the retention time and mass spectroscopic investigation the presence of *cis* and *trans* diastereomers could be ascertained. The stereochemistry of 1-*p*-menthene was established using specific rotation measurement. The specific rotation value for the starting material (*R*-limonene, 97%) is $[\alpha]_{\text{D}}^{22} +113.4$ (*c* 2.0, CH₂Cl₂). Whereas, specific rotation of the product is $[\alpha]_{\text{D}}^{22} +103.8$ (*c* 2.0, CH₂Cl₂), which matches with that of the *R* isomer of 1-*p*-menthene (87.9 % calculated from GC). Thus, the stereochemistry of the chiral center was preserved.

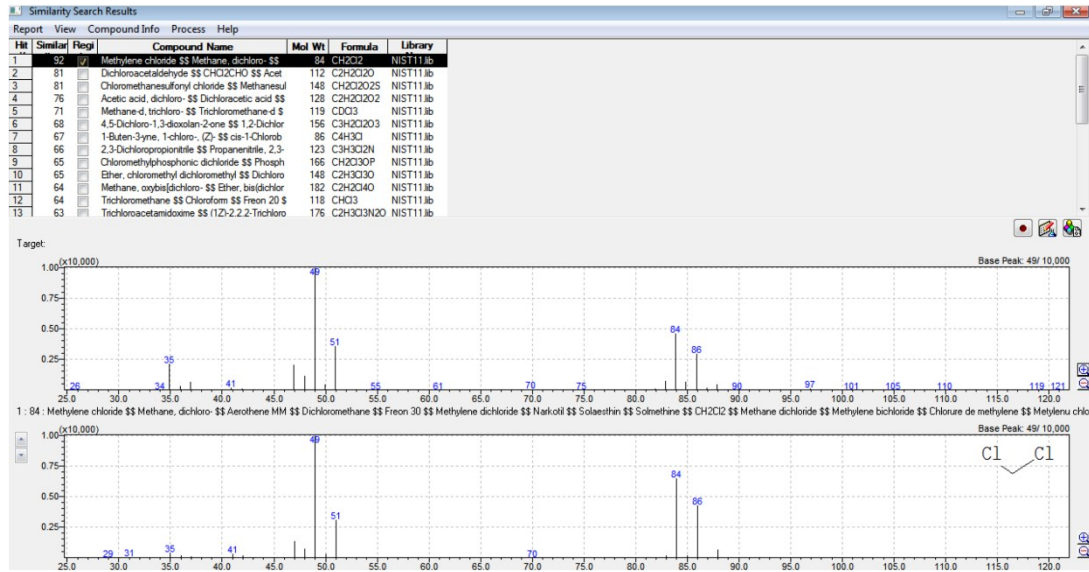
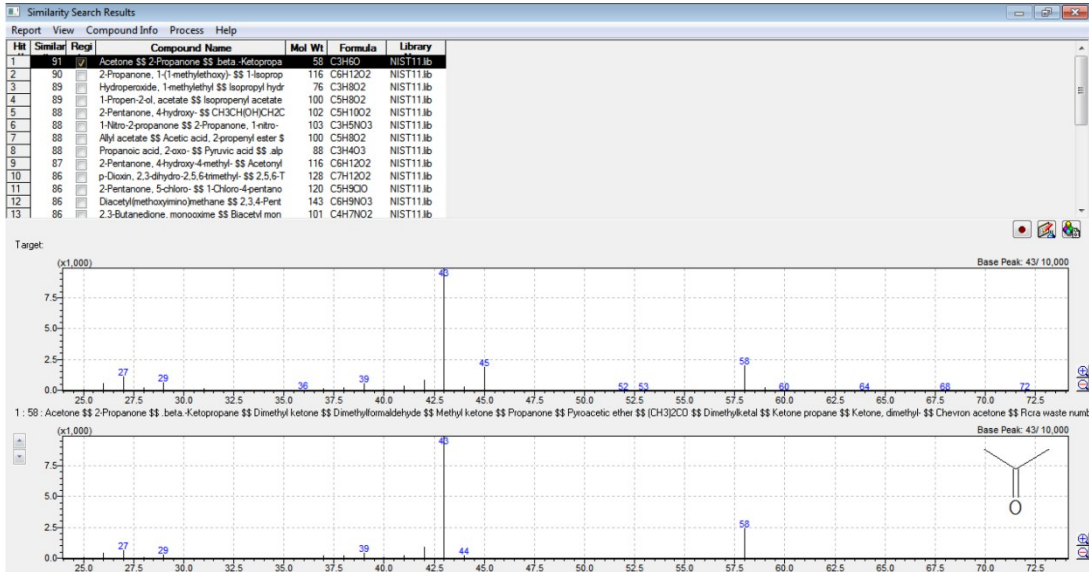
Table 2 entry 19 GC-MS plot



Similarity Search Results

Hit	Similar	Reg	Compound Name	Mol Wt	Formula	Library
1	92	<input checked="" type="checkbox"/>	Butane \$\$ n-Butane \$\$ Diethyl \$\$ Freon 600	58	C4H10	NIST11.lb
2	89	<input type="checkbox"/>	Pentane, 2-bromo- \$\$ 2-Bromopentane \$\$ 2-P	150	C5H11Br	NIST11.lb
3	88	<input type="checkbox"/>	Butane, 2-methyl- \$\$ iso-Pentane \$\$ 1,1,2-Tri	72	C5H12	NIST11.lb
4	87	<input type="checkbox"/>	Amyl nitrite \$\$ n-Pentyl nitrite \$\$ n-Amyl nitrite	117	C5H11NO2	NIST11.lb
5	87	<input type="checkbox"/>	Propane, 1-nitro- \$\$ 1-Nitropropane \$\$ n-C3H	89	C3H7NO2	NIST11.lb
6	86	<input type="checkbox"/>	Oxetane, 2,2-dimethyl- \$\$ Butane, 1,3-epoxy-3	86	C5H10O	NIST11.lb
7	86	<input type="checkbox"/>	1-Propanesulfonyl chloride \$\$ Propane-1-sulfo	142	C3H7O2S	NIST11.lb
8	86	<input type="checkbox"/>	Butane, 1-fluoro- \$\$ Butyl fluoride \$\$ 1-Fluorob	76	C4H9F	NIST11.lb
9	86	<input type="checkbox"/>	Heptane \$\$ n-Heptane \$\$ Dipropylmethane \$	100	C7H16	NIST11.lb
10	86	<input type="checkbox"/>	Pentanal, 2-methyl- \$\$ Valeraldehyde, 2-methy	100	C6H12O	NIST11.lb
11	85	<input type="checkbox"/>	Nitrous acid, butyl ester \$\$ n-Butyl nitrite \$\$ Bu	103	C4H9NO2	NIST11.lb
12	85	<input type="checkbox"/>	Butane, 1-isocyanato- \$\$ Isocyanic acid, butyl	99	C5H9NO	NIST11.lb
13	85	<input type="checkbox"/>	Isobutane \$\$ Propane, 2-methyl- \$\$ Trimethyl	58	C4H10	NIST11.lb





Catalyst recyclability test

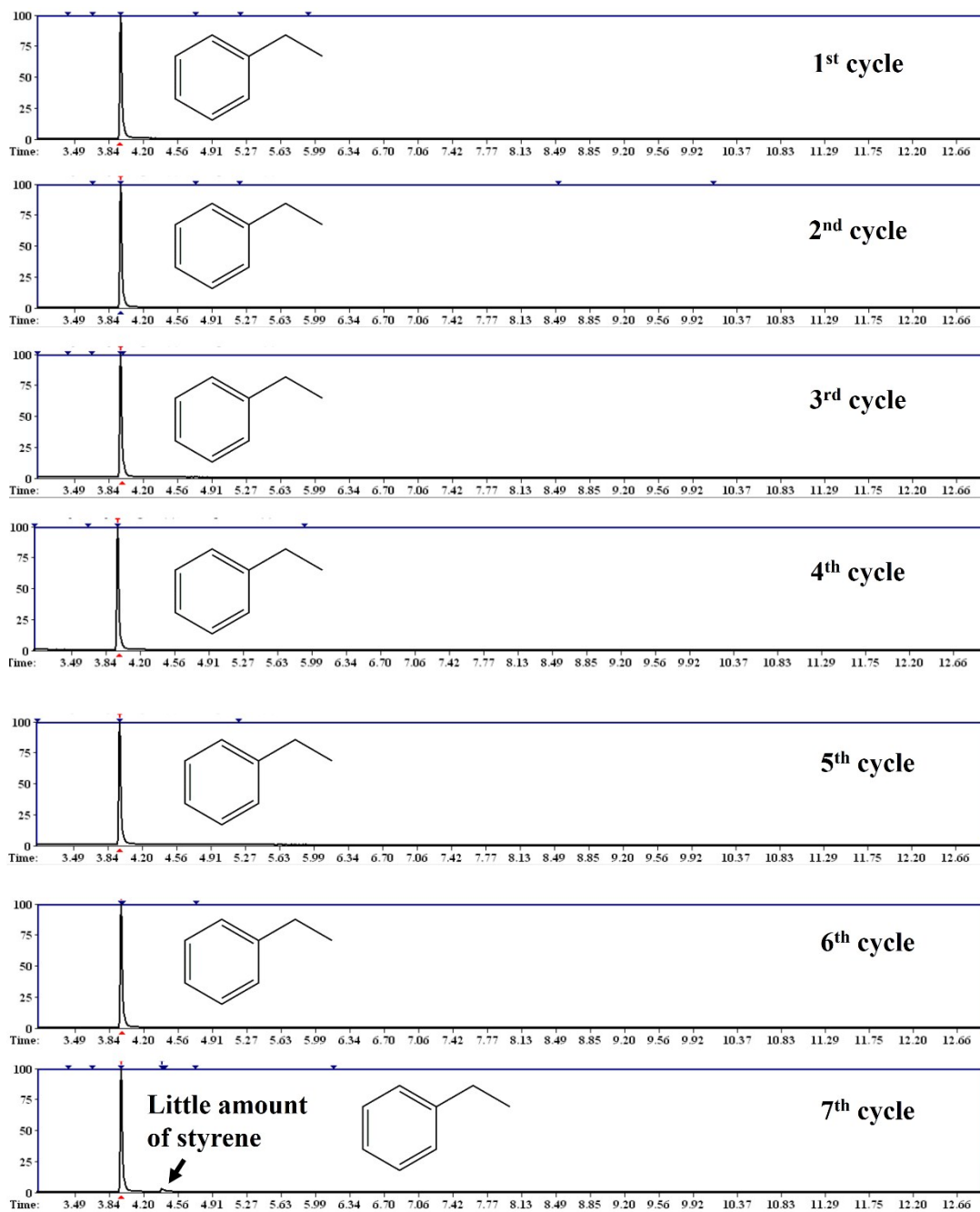
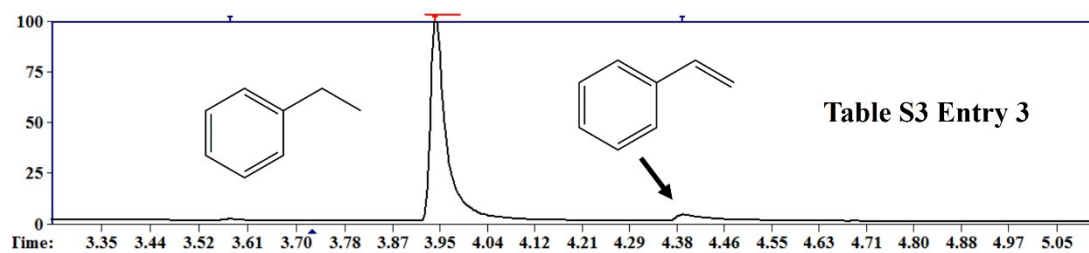
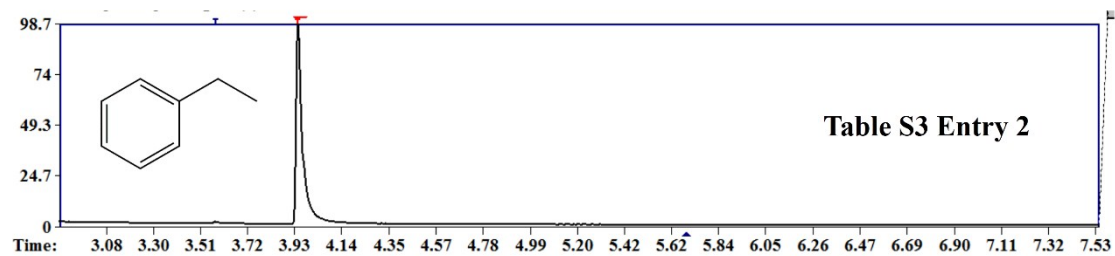
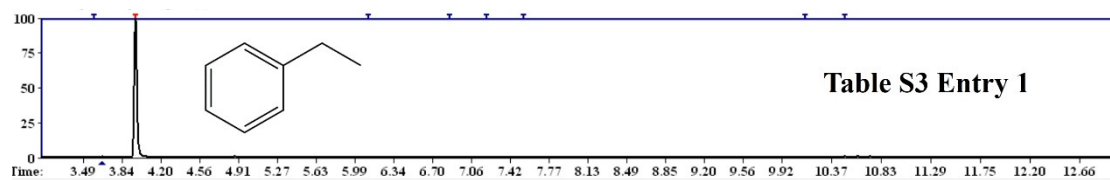
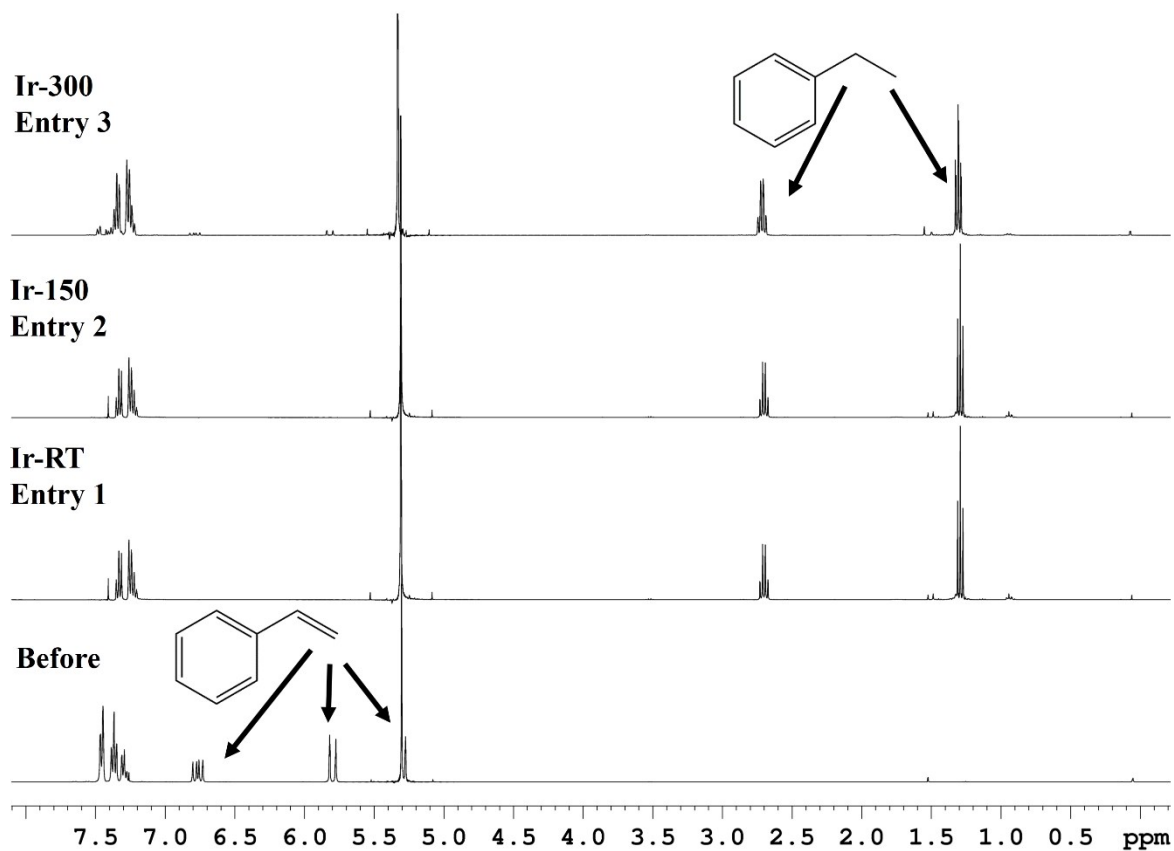
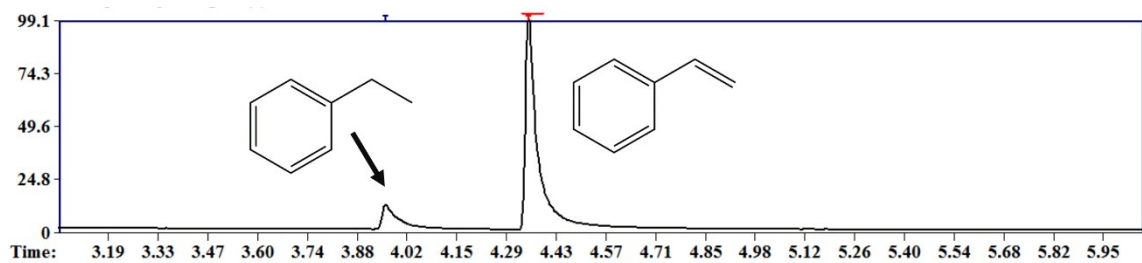
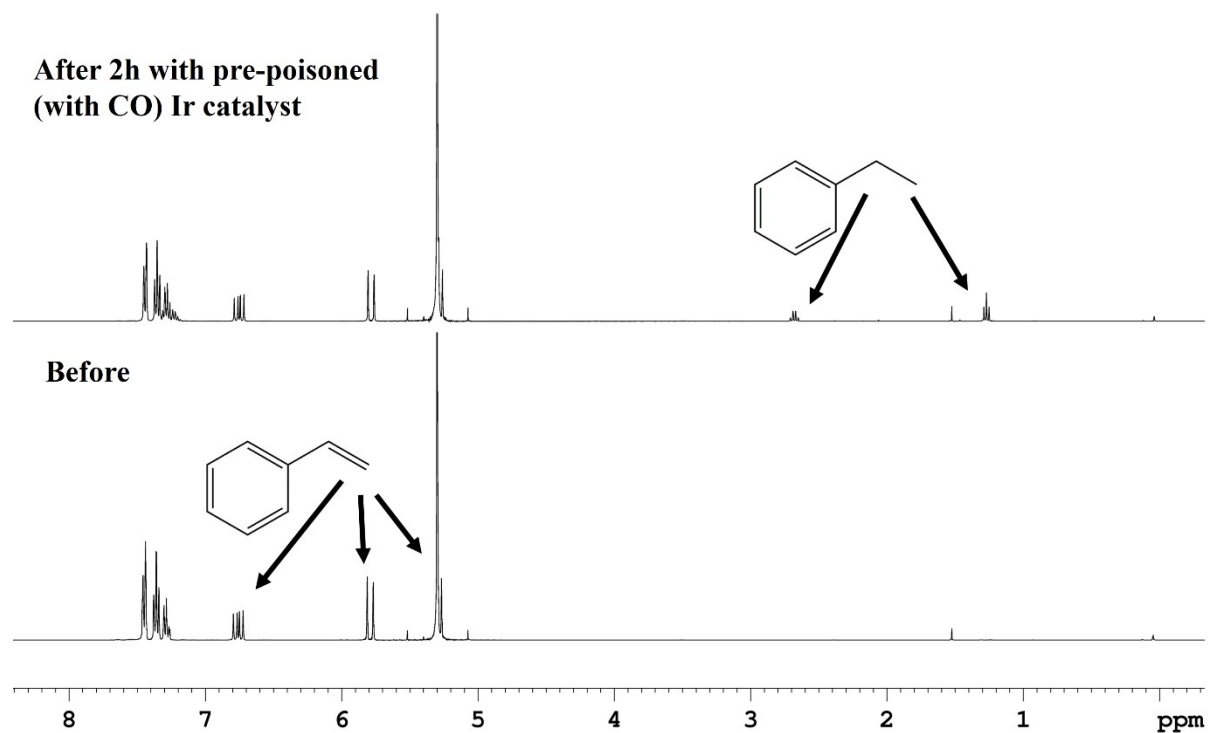


Table S3 (hydrogenation of styrene using annealed iridium nanosponges)



Catalyst poisoning experiment with CO

Hydrogenation of styrene using pre-poisoned iridium catalyst



Hydrogenation of styrene using post-poisoned iridium catalyst (with CO) after 1st step

2nd step - post-poisoned (with CO) Ir catalyst after 1st step then reaction carried out for 2 h

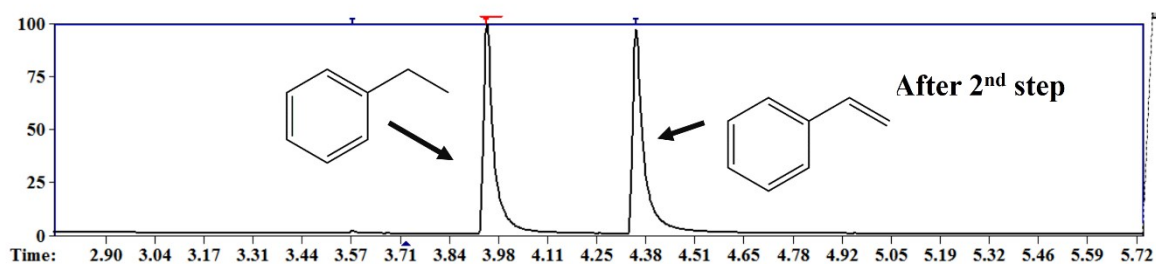
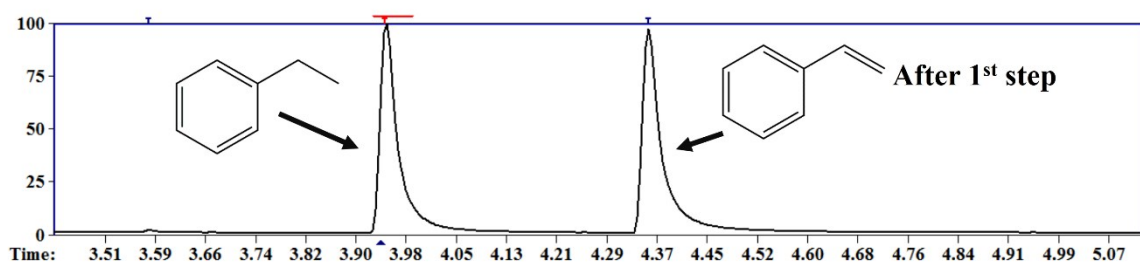
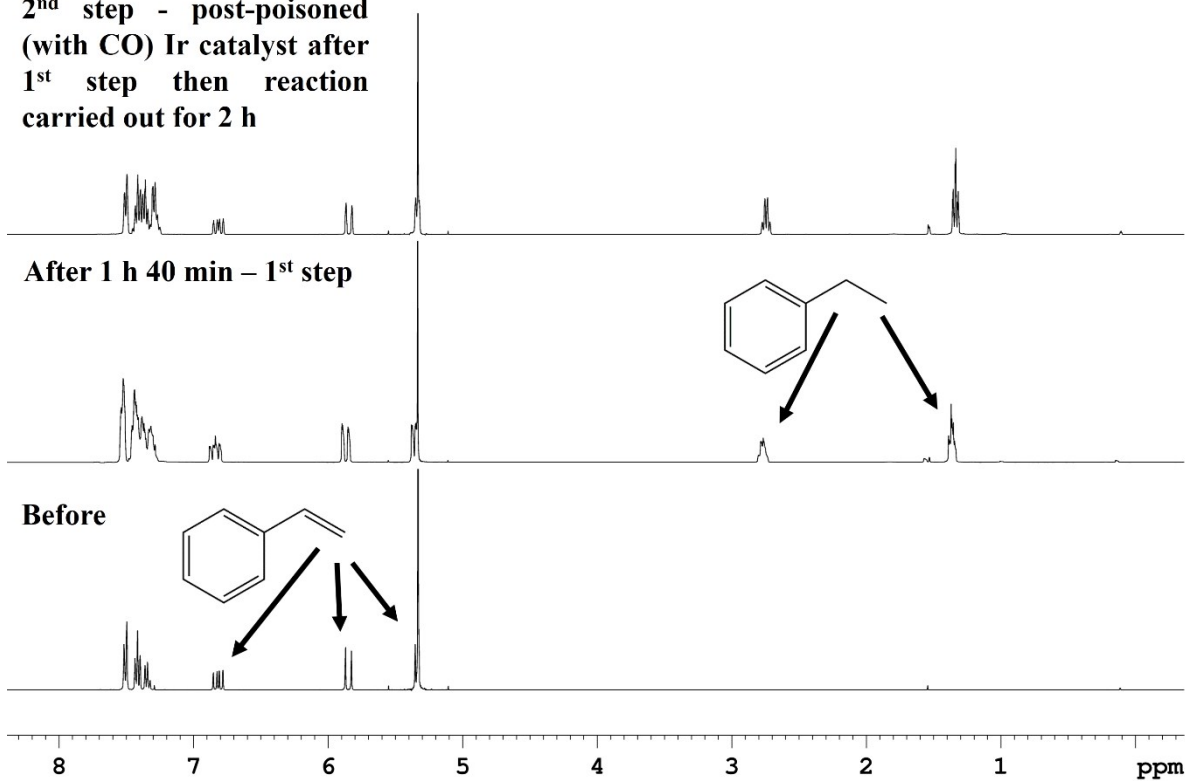


Table S4 (hydrogenation styrene with iridium nanospheres synthesized from different precursors)

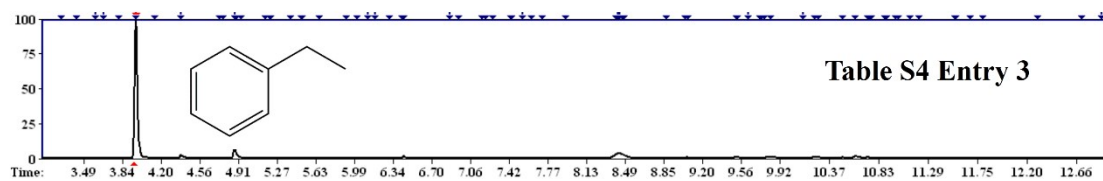
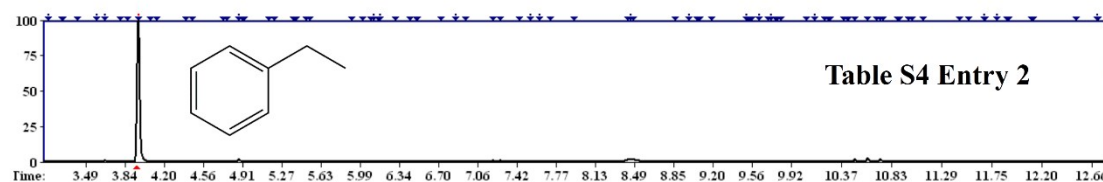
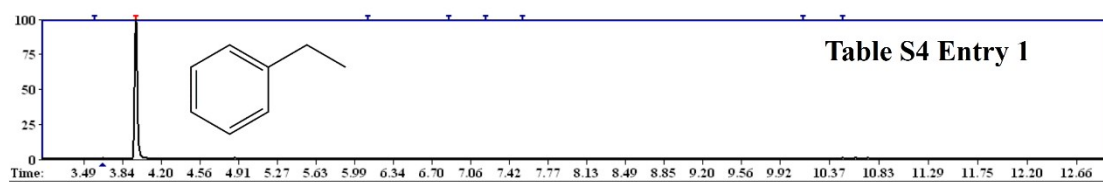
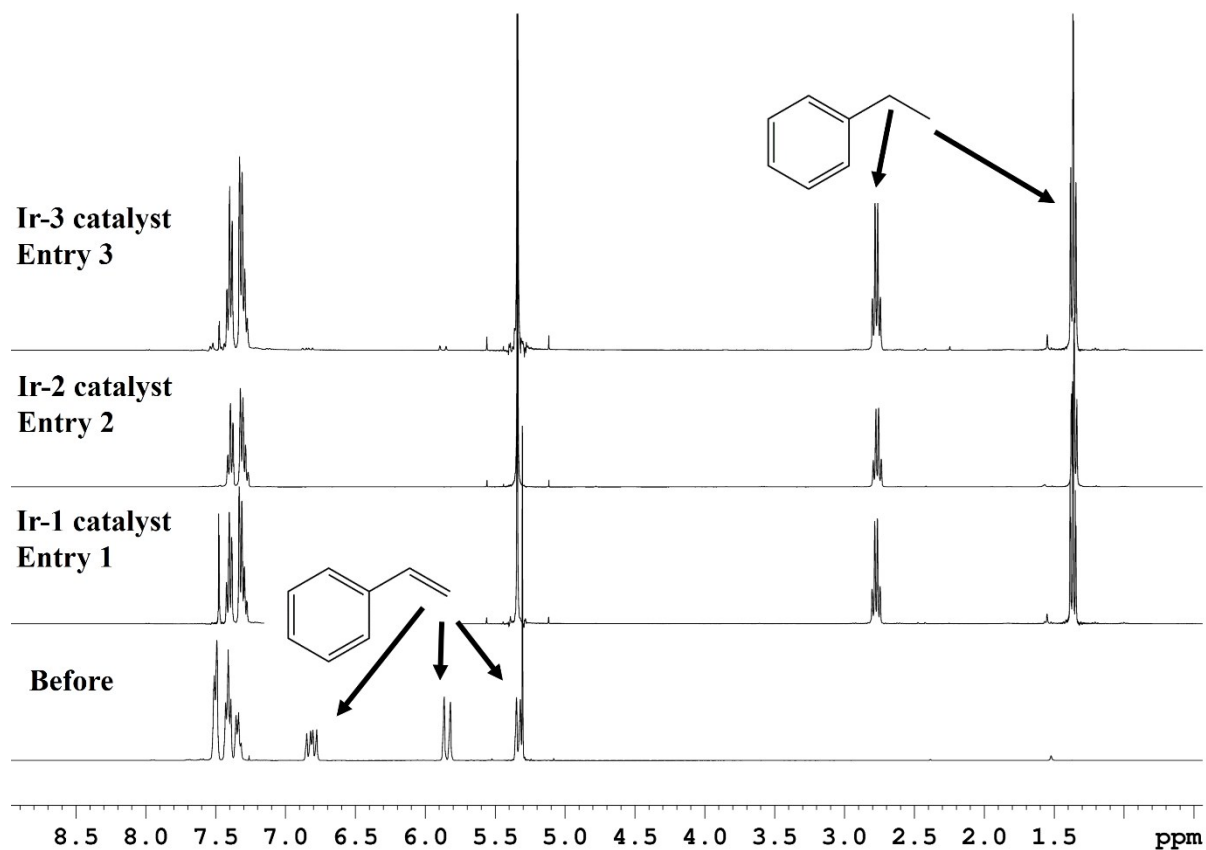


Table S4. Hydrogenation of styrene performed for 1 h using iridium nanosponge synthesized from different iridium precursors

Entry	Styrene/catalyst	Catalyst	Ratio of styrene to ethyl benzene ^a
1	2000	Ir from H ₂ IrCl ₆	53.6:46.4
3	2000	Ir from IrCl ₃ .xH ₂ O	53.9:46.1
5	2000	Ir from [Ir(COD)Cl] ₂	53.4:46.4

All reactions were carried out at 4 bar hydrogen gas pressure and at 30 °C in CH₂Cl₂ for 1 h; ^aconversion was determined by GC/MS analysis.

Table S4 ¹H-NMR stack plot

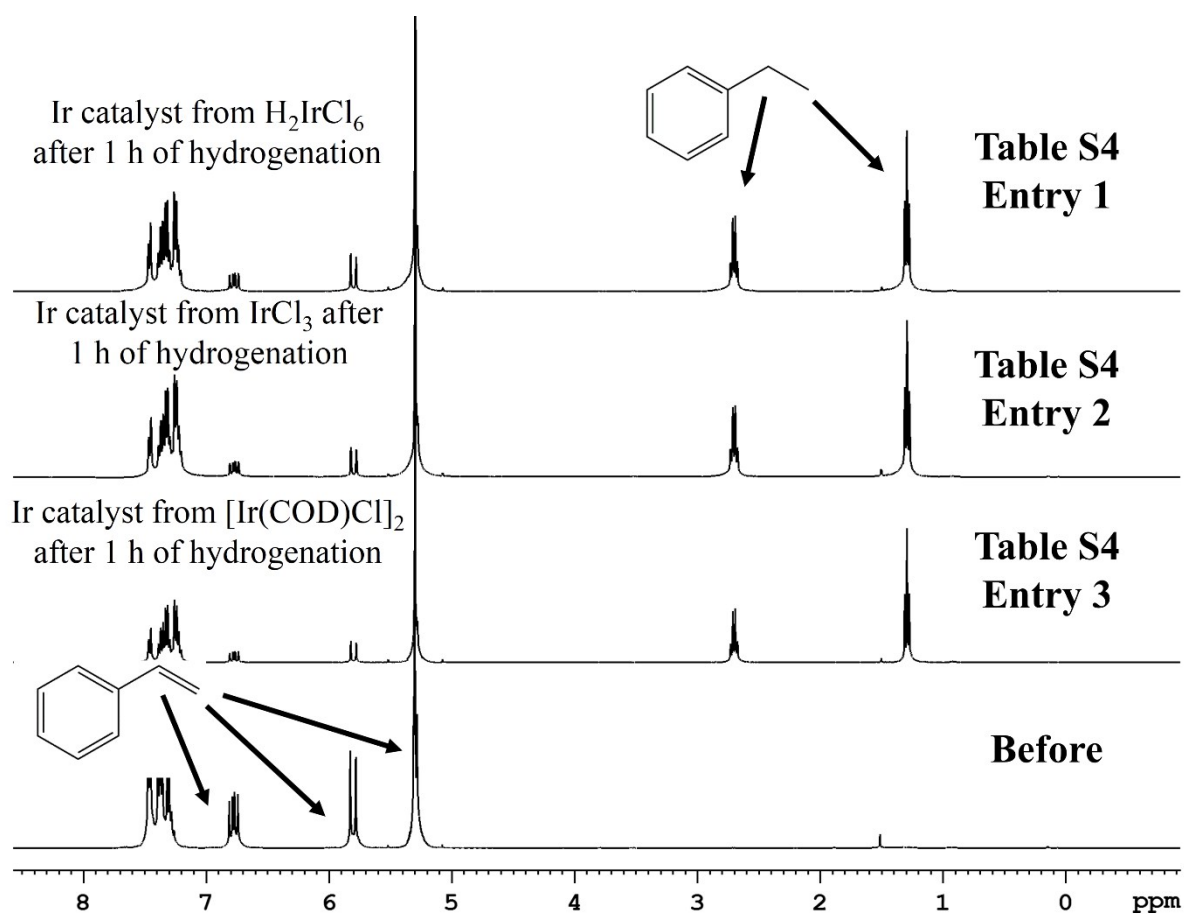


Table S4 GC stack plot

